energies

*Article*

# Advanced Exergo-Environmental Assessments of an Organic Rankine Cycle as Waste Heat Recovery System from a Natural Gas Engine

**Aldair Benavides Gamero †, Josué Camargo Vanegas, Jorge Duarte Forero, Guillermo Valencia Ochoa and Rafael Diaz Herazo ***

Efficient Energy Management Research Group-Kai, Universidad del Atlántico, Carrera 30 Número 8-49, Puerto Colombia, Barranquilla 080007, Colombia; aebenavides@mail.uniatlantico.edu.co (A.B.G.); jmiguelcamargo@mail.uniatlantico.edu.co (J.C.V.); jorgeduarte@mail.uniatlantico.edu.co (J.D.F.); guillermoevalencia@mail.uniatlantico.edu.co (G.V.O.)
* Correspondence: rediaz@mail.uniatlantico.edu.co; Tel.: +57-3506186998
† Deceased.

**Abstract:** This paper aims to present the real improvement opportunities of a simple organic Rankine cycle (ORC) as waste heat recovery system (WHRS) from the exhaust gases of a natural gas engine using toluene as the working fluid, based on the exergy and environmental point of view. From the energy and exergy balances, the advanced exergetic analysis was developed to determine the irreversibilities and opportunities for improvement. Since the traditional exergo-environmental analysis, it was found that the component with the greatest potential environmental impact associated with exergy (bF = 0.067 mPts/MJ) and per unit of exergy ($\dot{B}$D = 8.729 mPts/h) was the condenser, while the exergy-environmental fraction was presented in the turbine (52.51%) and pump-2 (21.12%). The advanced exergo-environmental analysis showed that the environmental impact is more associated with the operational behavior of the components, with 75.33% of the environmental impacts being of endogenous nature, showing that the environmental impacts are generated to a reduced magnitude through the interactions between components. However, it was identified that much of the environmental impacts in ITC 1 could be reduced, with 81.3% of these impacts being avoidable. Finally, the sensitivity analysis results revealed that steel is the material of the components with the least environmental impact.

**Keywords:** exergetic analysis; life cycle assessment; ORC; traditional/advanced environmental analysis; waste heat recovery system

check for updates

**Citation:** Benavides Gamero, A.; Camargo Vanegas, J.; Duarte Forero, J.; Valencia Ochoa, G.; Diaz Herazo, R. Advanced Exergo-Environmental Assessments of an Organic Rankine Cycle as Waste Heat Recovery System from a Natural Gas Engine. *Energies* **2023**, *16*, 2975. https://doi.org/10.3390/en16072975

Academic Editor: Andrea De Pascale

Received: 10 February 2023
Revised: 14 March 2023
Accepted: 18 March 2023
Published: 24 March 2023



## 1. Introduction

Due to the high demand for energy in recent years, the consumption of raw materials for non-renewable energy, such as natural gas, coal, oil, and other fossil fuels, has increased. As a result, environmental pollution caused by fossil energy consumption has increased significantly as reflected in the current environmental problems, making it a global concern. Several analyses have been carried out to show and evaluate the environmental impacts generated by energy generation systems [1]. However, in power generation system applications, life cycle assessments (LCA) based on Eco-Indicator 99 have become relevant in recent years due to their standardization in international criteria and their ease of application [2,3].

Life cycle assessment methodology allows the evaluation of the environmental impacts associated with a given process, a product, or an activity [4], which makes it possible to identify and quantify the use of material, energy, and environmental emissions produced, and thus determines its impact on the evaluation and creation of environmental improvement strategy [4]. Different life cycle analysis studies have been carried out in various applications, such as critical reviews in estimating environmental impacts on roads [5], research trends in construction using the method [6], and research on solar power plants, making comparisons with different methods of power generation [7]. In addition, accounting for resources and knowing irreversibilities, the applications of exergy analysis allow for the recording and identification of waste. It has been proposed that life cycle analysis can be integrated into exergy analysis to account for and evaluate the potential for reducing environment damage [8]. This has led to combinations of these approaches in thermal systems, such as cooling and hot water production for residential places, as well as implementations in solar energy-based systems for heating [9], comparisons for selecting the best methodology for resource recovery from household waste based on exergetic life cycle assessment [10], and the impact assessments of waste heat recovery systems (WHRS) using an exergetic basis to find environmental impacts and costs of the components that will be used in the energy conversion process, called exergo-environmental analysis [1].

Methodologies of exergo-environmental analysis have been proposed where it is considered that exergetic analysis cannot be replaced by other types of analysis, such as energy and materials, due to the importance of exergetic efficiency in this type of evaluation [8,11]. Several studies have been carried out in different systems with success in applications such as geothermal district heating systems [12], cogeneration plants [13], reformed methane steam processes for hydrogen production [14], and the combined thermodynamic cycle power plant based on chemical loop technology [15].

Despite its usefulness in identifying the substantial potential for improvement, the conventional exergo-environmental analysis has many important constraints, such as knowledge about the real potential for improvement and the interactions between components [16]. With this premise, many researchers have improved the traditional exergetic analyses, dividing the exergy destructions generated by the components into unavoidable/avoidable and endogenous/exogenous parts and breaking them down into avoidable exogenous/endogenous and unavoidable endogenous/exogenous parts [17]. This approach can be applied to the impacts associated with each component, creating another emphasis in this type of analysis, taking into account how and to what degree the changes in a system component affect the overall system performance and the environmental impact produced by the system components. This type of methodology is called advanced exergo-environmental analysis. The advanced exergo-environmental analysis is a relevant tool in diagnosing a system and evaluating the real potential for improvement by breaking down the avoidable and unavoidable parts [18,19].

Research has been done on exergo-environmental analysis, such as the case of Boyano et al. [20] which showed the use of conventional and advanced exergo-environmental analysis in a methane steam reformer plant, focusing on the reforming reactor. Petrakopoulou et al. [21] performed an advanced exergo-environmental assessment of a fuel power plant based on the $CO_2$ capture methodology. The results of the advanced exergo-environmental analysis showed that most of the impact of the system is unavoidable and endogenous. Emin Açıkkalp et al. [22] presented the application of exergo-environmental analysis of an electricity generation facility. The exergo-environmental factor was 0.277, and the environmental impact of the electricity was 8.472 mPts/h. Petrakopoulou et al. [23] developed an assessment of the environmental impact of a zero-emission advanced plant (AZEP), including the capture of $CO_2$ using advanced exergo-environmental analysis. Results suggested that the potential to reduce the environmental impact of the AZEP plant is restricted due to the avoidable low environmental impact due to several components' internal inefficiencies. Hong et al. [24] analyzed a supercritical coal power plant using two cases: one with $NO_x$, $SO_2$, and dust mitigation controls and the other without these controls. The result revealed that the destruction of endogenous exergy is the main reason the environmental impact of each component, except in components where the cycle is regenerated.

On the other hand, assessing the environmental impact of organic Rankine cycles is crucial to identify potential energy savings and thus reduce the environmental impact. The application of conventional energy analysis to power cycles has been widely reported in the literature. However, advanced exegetic analysis can identify improvements in exegetic performance that are usually limited within conventional analysis [25].

In this regard, Boyaghchi et al. [26] evaluated the performance of a novel solar-ORC system equipped with ejector refrigeration cycle. Exergy and exergo-environmental concepts were applied. Their results showed that the overall system had an exergo-environmental impact of 98. 99 Pts/h. In addition, it was found that the condenser was the equipment that had the highest contribution to the total exergo-environmental impact of the system (31.6–31.19% Pts/h). Ding et al. [27] conducted an exergo-environmental analysis of an organic Rankine cycle (ORC) using four working fluids: R134a, R227ea, R152a, and R245fa. According to their findings, R245fa was the most environmentally friendly option, with a minimal exergo-environmental impact using copper (83 mPts/h) and steel (70.06 mPts/h). In addition, the results showed that the environmental impact depends strongly on the type of equipment material and the type of fluid working. In this sense, the authors concluded that the evaporator and condenser were the equipment with the greatest contribution to the exergy-environmental impact. Similar results were reported by Alibaba et al. [28], who investigated a hybrid geothermal-solar power plant using an ORC layout applying energy concept: exergo-environmental and emergo-environmental analysis. The analysis of the geothermal-solar hybrid cycle revealed that the evaporator ($3.77 \times 10^{-6}$ Pts/s and $6.18 \times 10^{6}$ sej/s) and turbine ($3.27 \times 10^{-6}$ Pts/s and $6.37 \times 10^{8}$ sej/s) had the highest amount exergo and exergo-environmental impact. Boyaghchi et al. [29] proposed a multi-generation system incorporating a proton exchange membrane (PEM) electrolyzer and a two-stage organic Rankine cycle ORC equipped with a biomass gasification process and ejector refrigeration loop. The authors modeled the system using exergo-environmental analysis. It was found that the R245fa-R134a had the highest rate of improvement in exergo-environmental impact 32.4% (172.8 mPts/h) compared to its baseline condition (540 mPts/h).

Wang et al. [30] conducted an exergo-economic and exergo-environmental analysis of a multi-generation ORC system driven by geothermal source. The results revealed that the total exergy-environmental impact of the overall system was 201.29 mPts/h. They found that the steam generator is one of the equipment types with the highest exergo-environmental factor (f = 89.35%) and exergo-environmental impact (104.67 mPts/h). Aliaba et al. [31] conducted a conventional and exergo-environmental analysis of a geothermal-solar hybrid power plant using an organic Rankine cycle. The authors proposed two models: standalone geothermal-ORC (model 1) and geothermal-solar hybrid ORC (model 2). The exergo-environmental results for standalone geothermal-ORC (model 1) revealed that the turbine ($8.6 \times 10^{-6}$ Pts/s) and evaporator ($3.56 \times 10^{-6}$ Pts/s) represented the equipment that had the highest environmental impacts. Ghorbani et al. [32] integrated the internal reforming solid oxide fuel cell—gas turbine-ORC. The authors conducted an exergo-environmental analysis and found that the overall environmental impact can be reduced by decreasing the rate of exergetic destruction of the components, which requires more expensive materials and more efficient designs.

Advanced exergo-environmental analyses have also been applied to Rankine cycles coupled to internal combustion engines, as reported by Ochoa et al. [33]. In this work, the researchers modeled a recuperative organic Rankine cycle coupled to an internal combustion engine through an environmental and carbon footprint analysis. The authors analyzed different materials (aluminum, copper, and steel) in the construction phase on the system's environmental impact. The authors concluded that the material and equipment with the lowest environmental impact were steel and the turbine. Finally, Herrera-Orozco et al. [34] evaluated the waste heat recovery potential of a natural gas engine through an exergy-environmental analysis based on a regenerative organic Rankine cycle (RORC) and simple organic Rankine cycle (SORC). The authors used three working fluids: toluene, cyclohexane, and acetone. The results showed that the SORC/toluene configuration had the lowest values in the climate change category ($1.77 \times 10^{-3}$ kg $CO_2$ eq/kWh).

Based on the above, there is evidence of an increase in the application of advanced exergo-environmental analysis in ORC systems using different thermal sources; solar and geothermal sources being the most reported. However, only some studies have considered applying advanced exergo-environmental methodologies in waste heat recovery from internal combustion engines (ICE) using Rankine cycle. Furthermore, it is pertinent to highlight that internal combustion engines are one of the largest consumers of fossil fuels [35–37]. This implies that significant efforts should be made to identify exergy performance improvement opportunities that cannot normally be identified using conventional exergy analysis. In this way, it contributes to reducing the specific fuel consumption and greenhouse gas emissions. Therefore, this research presents an advanced exergo-environmental analysis of WHRs using ORC from the exhaust gases of a natural gas generation engine widely used in industrial applications worldwide, which allows increasing the energy and exergy performance of the thermal power system attending to a sustainable energy solution. The implementation of advanced methods to determine variables of greater importance for the performance improvement of the system based on energy and environmental criteria is presented. The main objective of this work is to provide engineers with additional information that will help better understand the design and operation of waste heat recovery (WHR) systems in stationary power generation engines, which conventional methods cannot obtain.

## 2. Materials and Methods

### *2.1. Cycle Description*

The proposed and studied configuration is shown in Figure 1. Figure 1a shows the thermodynamic points of the process. Figure 1b shows that the internal combustion engine supplies an air-natural gas mixture, which is compressed when it enters the cylinders [23]. The exhaust gases are expanded by a turbocharger (S1 flow), pass energy to the thermal oil (S5 flow) through the heat exchanger 1 (ITC1), and are then discharged into the atmosphere (S2 flow). The thermal oil circulates in its own circuit, which circulates through the energy supplied by pump-1 (P1), the hot fluid leaving ITC1 (S3 flow) operates a thermal source for preheating, evaporating, and reheating the organic fluid (toluene) through the evaporator, reaching the maximum pressure and temperature values in the ORC cycle at the turbine inlet (S6 flow). Then, the organic fluid enters the turbine where it expands, and generates work. The pressure of the organic fluid decreases to its lowest point, then it goes to the cooling stage (flow S7 to flow S7g) and condensation stage (flow S7g to S8). In the condensation process, cooling water was used, which absorbs heat from the working fluid. The heat gained by the water is released when it comes in contact with the medium. Finally, pump-2 (P2) is responsible for driving the working fluid to the evaporator (flow S9) at the evaporation pressure of the system, thus completing the cycle.

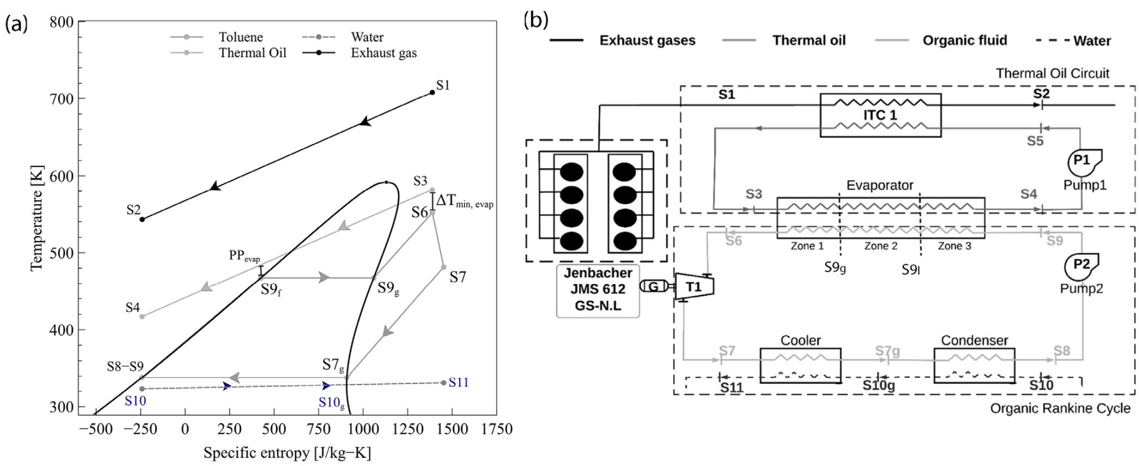


**Figure 1.** Scheme proposed (**a**) T−S diagram, (**b**) Waste heat recovery system.

The exhaust gas stream came from an industrial internal combustion engine (Jenbacher JMS 612 GS-N.L). The fuel composition consisted of methane (97.97%), nitrogen (1.50%), ethane (0.25%), and carbon dioxide (0.16%). The fuel uncorrected volume ratio is between 110–149 L/s. The composition of the exhaust gas was: $O_2$ (9.45–10.52% $v/v$), CO (588–731 mg/m$^3$), $NO_x$ (461–468 mg/m$^3$), $NO_2$ (317–368 mg/m$^3$), and NO (65–95 mg/m$^3$). The exhaust gas temperature is between 420–460 °C. The main operating parameters of the engine are shown in Table 1.

**Table 1.** Main engine characteristics.

| Descriptions | Value | Unit |
|---|---|---|
| Compression ratio | 710.5 | - |
| Number of cylinders | 12 | En V 60° |
| Maximum load capacity | 1982 | mm |
| Maximum torque | 60.66 | kN·m |
| Power at nominal speed | 1820 | kW |
| Engine speed | 1500 | $m^{-1}$ |
| Nominal speed | 1500 | rpm |
| Fuel mass fuel | 432 | kg/h |
| Exhaust mass flow | 9986 | kg/h |

### 2.2. Working Fluid Selection

In this section, the suitable working fluid for the system was selected, considering its thermo-physical properties compatible with the required operating conditions. Table 2 shows the criteria used for the choice of the working fluid to analyze its performance in the proposed configuration [38,39]. It is important to highlight that the choice of the working fluid is fundamental for the analysis of the organic Rankine cycle since its properties impact both the energy and exergy performance of the system, as well as the sizing of the components and their environmental impact [40].

**Table 2.** Selection criteria of the working fluid.

| No | Criteria | Operational Parameter | Reference |
|---|---|---|---|
| 1 | Critical temperature | >250 °C | [41] |
| 3 | Global Warming Potential (GWP) | <2000 | [42,43] |
| 4 | Ozone Depletion Potential (ODP) | 0 | [42] |
| 5 | Safety classification (NFPA 704 standard) | Class 4 not allowed | [44] |

Currently, research is focused on selecting working fluids in ORC systems to ensure optimal performance in terms of safety, environment, and cost [45]. Studies have also been conducted on different working fluids in ORCs coupled to internal combustion engines (ICEs) under different operating conditions [46,47]. In ORC-ICE applications with high source temperature (Tsource > 350), alkanes have been considered as working fluids [41], [48], as well as alcohols, aromatics, and siloxanes [49,50]. Therefore, alkanes are an excellent choice as working fluids in ORC systems because they are hydrocarbons with a vaporization temperature close to environmental temperature, allowing condensation at near-atmospheric pressure, and their critical conditions are favorable for working in high-temperature ORC systems [51]. Additionally, alkanes are environmentally friendly, with zero ODP and relatively low GWP [42].

Table 3 shows the thermophysical and environmental properties of toluene, which was selected as the working fluid, considering the criteria presented in Table 2. Chlorofluorocarbons (CFCs) and hydrochlorofluorocarbons were not considered due to their environmental effects according to the Montreal Protocol [52], as well as hydrofluorocarbons (HFCs) due to their high GWP values according to the Kyoto Protocol [53]. In this sense, and based on previous studies at ORC [51,54], toluene was selected as a suitable working fluid for the system.

**Table 3.** Thermophysical properties of the working fluid.

| Working Fluid | Type | $P_{crit}$ [MPa] | $T_{crit}$ [°C] | NFPA 704 | | ODP | GWP |
|---|---|---|---|---|---|---|---|
| | | | | Flammability | Health Hazard | | |
| Toluene | Dry | 4.13 | 319 | 3 | 2 | 0 | 2.7 |

### 2.3. Thermodynamic Modelling

This study applies a waste heat recovery system as a bottoming cycle couple to 2-MW stationary internal combustion engine. The proposed system uses a thermal oil circuit (Terminol-66) to properly integrate the heat source (exhaust gas) and the ORC and to maintain stable conditions in the evaporator. The simulation was done in Matlab 2018. The thermo-physical and transport properties were obtained using REFPROP 8.1 [55].

#### 2.3.1. Energy and Exergy Balance

To complete the energy analysis of the system, the pressure, temperature, and enthalpy have to be determined for every thermodynamic state. Therefore, the analysis was based on the thermodynamic modeling of each system component. This modeling was done by using the energy balance (Equations (1) and (2)) and the exergy balance in Equation (3).

$$\sum \dot{m}_{in} - \sum \dot{m}_{out} = 0 \tag{1}$$

$$\sum \dot{m}_{in} h_{in} - \sum \dot{m}_{out} h_{out} + \sum \dot{Q} + \sum \dot{W} = 0 \tag{2}$$

$$\sum \dot{m}_{in} \dot{X}_{in} - \sum \dot{m}_{out} \dot{X}_{out} + \dot{Q}\left(1 - \frac{T_0}{T}\right) - \dot{W} - \dot{X}_D = 0 \tag{3}$$

In subsequent analyses, it should be noted that the other parameters can be changed differently with each input adjustment that is produced, so it is necessary to determine the device inputs and outputs correctly.

#### 2.3.2. Exergy Analysis

The exergy analysis is developed to observe the useful energy of the flows since the qualitative evaluation of the energy is not possible with thermodynamic modeling. Three categories of exergy flows can be found: material, work, and heat. Physical exergy can be calculated from the values belonging to the material flows, as shown in Equation (4).

$$e^{ph} = (u - u_0) + P_0 \cdot (v - v_0) - T_0 \cdot (s - s_0) \tag{4}$$

Likewise, chemical exergy can be determined with Equation (5). The amount of chemical exergy can be considered necessary when a flow differs from its normal environmental conditions, according to Equation (5).

$$e^{ch} = \sum_{i=1}^{n} X_i \cdot \bar{e}_i^{CH} + RT_0 \sum_{i=1}^{n} X_i \cdot ln X_i \tag{5}$$

The specific exergy streams must be multiplied by their mass flow rate to obtain the exergy flow rate of the material flows, as shown in Equation (6).

$$\dot{E}_k = \dot{m}_k \cdot e_k \tag{6}$$

A system's components with high irreversibility can be identified through an exergetic analysis, as was studied in several investigations [56]. By establishing the exergy of the product $\dot{E}_{P,k}$ for any $k$ component, and exergy fuel for the $k$ component $\dot{E}_{F,k}$, its exergetic efficiency could be determined from Equation (7).

$$\epsilon_k = \frac{\dot{E}_{P,k}}{\dot{E}_{F,k}} \quad (7)$$

The exergy destruction fraction is a helpful variable for comparing the different variables, as defined in Equation (8).

$$y_{D,k} = \frac{\dot{E}_{D,k}}{\dot{E}_{F,sys}} \quad (8)$$

where $\dot{E}_{D,k}$ is the exergy destruction inside the $k$-component and $\dot{E}_{F,sys}$ is the exergy of the fuel supplied to the system. The term $y_{D,k}$ is a measurement of the exergy destruction contribution inside the $k$-component to reduce the energy performance of the whole system.

### 2.4. Advanced Exergetic Analysis

Although traditional exergetic analysis provides information on the components with the greatest irreversibility in the system, the information is not sufficient to use strategies that allow for better performance in the plant. Advanced exergetic analysis can illuminate the steps in engineering and design for the operation and design of more efficient systems. Through advanced analysis, the previously calculated exergy destruction is disaggregated into partly avoidable and unavoidable, equally into partly endogenous and exogenous, which could be divided into endogenous avoidable/unavoidable and exogenous avoidable/unavoidable.

#### 2.4.1. Graphic Method

For an ideal system with a consistent product exergy $E_{P,tot}$. According to Kelly [57], the exergy balance can be described as shown in Equation (9).

$$E_{P,tot} = \dot{E}_F^{if} - \dot{E}_L^{if} \quad (9)$$

However, in the presence of irreversibilities in the $k$th component, an increase in the required input exergy will be found ($\dot{E}_F{}^{k}$), and there will also be an increase in lost exergy ($\Delta\dot{E}_L{}^{k}$). When the destroyed exergy is only produced by the component studied, it is called endogenous destroyed exergy, so that Equation (9) becomes Equation (10).

$$\dot{E}_{P,tot} + \dot{E}_{D,k} = \left(\dot{E}_{F,tot}{}^{id} + \dot{E}_{F,tot}{}^{k}\right) - \left(\dot{E}_{L,tot}{}^{id} + \dot{E}_{L,tot}{}^{k}\right) \quad (10)$$

However, when the destroyed exergy is also present in the other components, Equation (10) is rewritten as shown below:

$$\dot{E}_{P,tot} + \dot{E}_{D,k} + \dot{E}_{D,others} = \left(\dot{E}_{F,tot}{}^{id} + \dot{E}_{F,tot}{}^{RS}\right) - \left(\dot{E}_{L,tot}{}^{id} + \dot{E}_{L,tot}{}^{RS}\right) \quad (11)$$

where $\dot{E}_{F,tot}{}^{RS}$ is the required input exergy and $\dot{E}_{L,tot}{}^{RS}$ represents the increase in the exergy lost due to the destruction of exergy in all its components. If all of the other components function ideally (without irreversibility) the $\dot{E}_{D,others}$ tends to be zero (or minimal). Given that the exergy destroyed endogenously is a function of the energy efficiency of the component, its exergetic efficiency must remain constant, while the exergy destroyed from the other components varies, graphically presenting a straight line, as shown in Figure 2.

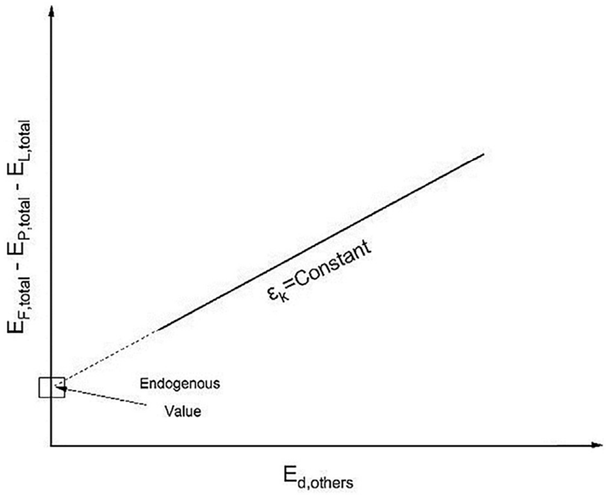


**Figure 2.** Value of exergy destroyed endogenously by the graphic method.

Figure 2 represents the total exergy destruction of the system due to the destruction of exergy in the other components, with the exception of component $k$. Thus, the intersection of the slope with the vertical axis will show the value of the destruction of the endogenous exergy of the $k$th-component, which occurs when $E_{D,others} = 0$ or when $E_{D,others} =$ minumun for the other components.

2.4.2. Exogenous and Exogenous Destroyed Exergy

For a system of n components, the destruction of the endogenous exergy $\dot{E}_D{}^{EN}$, is the destruction of exergy connected with the operation of the k-component, which occurs where the component operates under actual conditions, and all the remaining components of the system operate with no irreversibility (ideally). The output power of the system remains constant in all estimates. The ideal and unavoidable conditions for the components are shown in Table 4.

**Table 4.** Real, ideal, and unavoidable conditions for the ORC cycle. Adapted from [33].

| Component | Real | Ideal | Unavoidable |
|---|---|---|---|
| Turbine | $\eta_{iso} = 0.8$ | $\eta_{iso} = 1$ | $\eta_{iso} = 0.95$ |
| Pumps | $\eta_{iso} = 0.75$ | $\eta_{iso} = 1$ | $\eta_{iso} = 0.95$ |
| Condenser | $\Delta T_{min} = 15$<br>$\Delta P = 1\%$ | $\Delta T_{min} = 0$<br>$\Delta P = 0\%$ | $\Delta T_{min} = 3$<br>$\Delta P = 0.5\%$ |
| Evaporator | $\Delta T_{min} = 35$<br>$\Delta P = 2\%$ | $\Delta T_{min} = 0$<br>$\Delta P = 0\%$ | $\Delta T_{min} = 3$<br>$\Delta P = 1\%$ |

The exergy destruction was calculated using the graphical method for significant components of the cycle. The exogenous exergy destruction is calculated after evaluating the endogenous exergy destruction of the $k$th-component by subtracting the endogenous exergy destruction from the actual exergy. The exogenous destruction of an exergy $\dot{E}_D{}^{EX}$ is the exergy destruction imposed on the $k$th-component through the operation of the remaining components that make up the overall system, as denoted in Equation (12).

$$\dot{E}_{D,k} = \dot{E}_{D,k}{}^{EN} + \dot{E}_{D,k}{}^{EX} \tag{12}$$

Even when technical improvements are made to system components, due to technological and economic limits, there will always be a portion of exergy devastation that cannot be stopped. Such destruction of exergy, which cannot be minimized, is called irreversible death of exergy. Then, by implementing these technological improvements, exergy will be called avoidable loss of exergies. The exergy destroyed in a component is defined as shown in Equation (13).

$$\dot{E}_{D,k} = \dot{E}_{D,k}^{\;AV} + \dot{E}_{D,k}^{\;UN} \tag{13}$$

The unavoidable exergy can be calculated using Equation (9), where $\dot{E}_{D,k}^{\;UN}$ is the total unavoidable exergy [58].

$$\dot{E}_{D,k}^{\;UN} = \dot{E}_{P,k} \cdot \left(\frac{\dot{E}_{D,k}}{\dot{E}_{P,k}}\right)^{UN} = \dot{E}_{P,k} \cdot \left(\frac{1}{\varepsilon_k{}^{UN}} - 1\right)^{UN} \tag{14}$$

To determine the unavoidable exergy destroyed, an endogenous curve must be constructed for each component, in which endogenous exergy destroyed is calculated for each component by varying its exergetic efficiency, as seen in Figure 3, where $\dot{E}_{D,k}^{\;EN,UN}$ is the unavoidable endogenous exergy of a $k$th-component and $\epsilon_k$ is the exergetic efficiency of the $k$th-component.

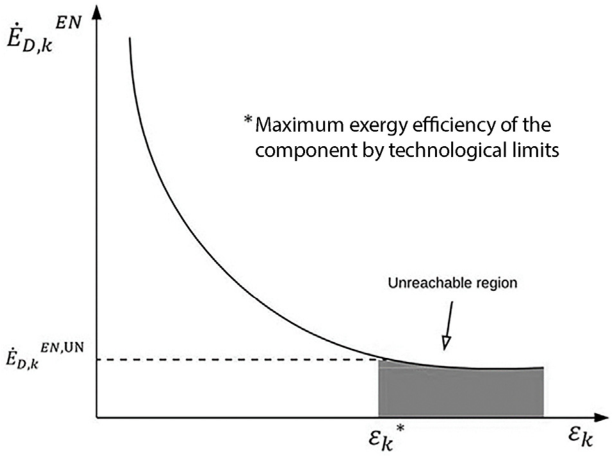


**Figure 3.** Endogenous curve by the graphic method.

Using the endogenous curve, the unavoidable endogenous exergy loss of each of the components that make up the device can be calculated; the avoidable endogenous exergy devastation can be determined by subtracting the value of the overall exergy of the component from the value of the unavoidable exergy destroyed, as shown in Equation (15) [58,59]

$$\dot{E}_{D,k}^{\;EN} = \dot{E}_{D,k}^{\;EN,AV} + \dot{E}_{D,k}^{\;EN,UN} \tag{15}$$

By integrating the avoidable and unavoidable concept with the concept of endogenous and exogenous, it is possible to divide into four specific parts of destroyed exergies for better analysis.

#### 2.4.3. Exogenous and Exogenous Destroyed Exergy

Using the concept described in this section, it is possible to divide it into four parts using the concept of avoidable/unavoidable to determine the technological limits for each component [26]. Using Equation (16), it is possible to find the destruction of avoidable endogenous exergy, which is the exergy destroyed in the $k$th-component [58,59]:

$$\dot{E}_{D,k}^{\;EN,AV} = \dot{E}_{D,k}^{\;EN} - \dot{E}_{D,k}^{\;EN,UN} \tag{16}$$

So, the unavoidable exergy destruction can be found in the component, as reflected in Equation (17) [58,59]:

$$\dot{E}_{D,k}^{\;UN} = \dot{E}_{D,k}^{\;EX,UN} + \dot{E}_{D,k}^{\;EN,UN} \tag{17}$$

Therefore, it is possible to find the destruction of unavoidable exogenous energy, which is the unavoidable portion of the k-component generated by the other system components, as denoted in Equation (18).

$$\dot{E}_{D,k}{}^{EX,UN} = \dot{E}_{D,k}{}^{UN} + \dot{E}_{D,k}{}^{EN,UN} \tag{18}$$

So, it is possible to find the destruction of exogenous exergy in the *k* component, described in Equation (19) [58,59]:

$$\dot{E}_{D,k}{}^{EX} = \dot{E}_{D,k}{}^{EX,AV} + \dot{E}_{D,k}{}^{EX,UN} \tag{19}$$

As shown in Equation (19), it is possible to find a relationship to find the avoidable exogenous exergy destruction in the k component, which is the exergy that can be reduced in the k component caused by the other components, as shown in Equation (20):

$$\dot{E}_{D,k}{}^{EX,AV} = \dot{E}_{D,k}{}^{EX} + \dot{E}_{D,k}{}^{EX,UN} \tag{20}$$

With this, it is possible to find the destruction of total exergy, according to Equation (21):

$$\dot{E}_{D,k} = \dot{E}_{D,k}{}^{EX,AV} + \dot{E}_{D,k}{}^{EX,UN} + \dot{E}_{D,k}{}^{EN,AV} + \dot{E}_{D,k}{}^{EN,UN} \tag{21}$$

### *2.5. Life Cycle Assessment (LCA)*

To evaluate the potential environmental impacts of the ORC at each stage of the cycle, the LCA (life cycle analysis) methodology is performed [24], which evaluates and describes in great detail the mass, energy, and exergy flows at each stage of the cycle, and is detailed graphically as shown in Figure 4. The procedure is carried out through the considerations to be taken in the ISO 14000 environmental management standard, which is standardized the Eco-Indicator 99 methodology [60]. The environmental impact of the components, which are distributed by flows, are classified according to the phase in which they are found: construction, operation and maintenance, and decommissioning [61] as can be seen in Figure 4. Research has indicated that the loss of working fluid in an ORC system is estimated at between 0% and 2%. For a total operation of 20 years, an annual loss of 0.5% is estimated, which means that total losses will be 10% [27]. For the decommissioning phase, a fluid loss of 3% is estimated for operation.

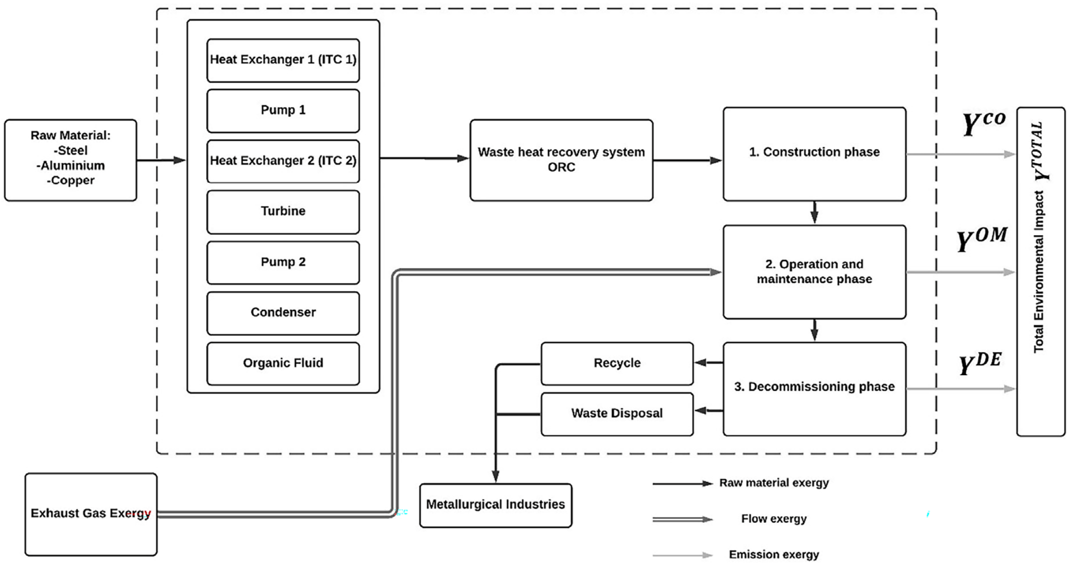


**Figure 4.** Life cycle assessment workflow.

For the impact assessment, the heat transfer area of a shell and tube heat exchanger (ITC1), was calculated by applying an energy balance to the equipment, as shown in Equation (22).

$$A_{ITC1} = \frac{Q}{U \cdot \Delta t} = \dot{m}_{s1} \cdot Cp_{s1} \cdot (T_{s1} - T_{s2}) = \dot{m}_{s5} \cdot Cp_{s5} \cdot (T_{s3} - T_{s5}) \tag{22}$$

where $U$ represents the average heat transfer coefficient in $kW/m^2 \cdot K$ and $\Delta t$ is the calculated temperature difference, as shown in Equation (23).

$$\Delta T = F_T \cdot LMTD \tag{23}$$

where $F_T$ is a correction factor calculated, as shown in Equation (24).

$$F_T = \frac{\sqrt{R^2+1} \cdot ln \frac{1-S}{1-S \cdot R}}{(R-1) \cdot ln \frac{2-(S \cdot R + S - S \cdot \sqrt{R^2+1})}{2-(S \cdot R + S + S \cdot \sqrt{R^2+1})}} \tag{24}$$

where $R$ is the coefficient of effectiveness, and $S$ is the ratio of the heat capacity. The *log* means temperature difference *LMTD* is calculated, as shown in Equation (25).

$$LMTD = \frac{(T_{s1} - T_{s3}) - (T_{s2} - T_{s5})}{ln\left[\frac{(T_{s1} - t_{s3})}{(T_{S2} - T_{s5})}\right]} \tag{25}$$

However, for calculating the evaporator plate and the condenser, the proposed thermal and hydraulic model was used for each operation phase in this equipment [62]. For the two components previously mentioned, the mass was calculated according to Equation (26) [27].

$$M_k = \rho \cdot A_k \cdot \delta \tag{26}$$

where $M_k$ is the mass of the evaporator and condenser (kg), $\rho$ is the density of the material ($kg/m^3$), $A_k$ is the heat transfer area of the equipment, and $\delta$ is the thickness of the material (m). The material thickness (δ) was assumed to be 0.002 m [27]. For the rest of the components, such as pumps and turbines, different studies have defined the mass as a function of the power consumed and generated, respectively, as shown in Equation (27) below [27].

$$M_k = \alpha \cdot W_k \tag{27}$$

where α is the necessary material quality per kW of power, and where $W_k$ is the power consumed for the pumps and generated for the turbine. In this work, it was assumed that the amount of material required for the pump in the construction phase was 14 kg/kWh; while for the turbine, the value was 1.22 kg/kWh [27].

The environmental impact of the components of the system was calculated by Equation (28).

$$Y_k = M_k \cdot \varphi_k \tag{28}$$

where $\varphi_k$ is the value of Eco-99 coefficient in the construction phase of steel (86 mPts/kg) and copper (1400 mPts/kg) [27].

The Environmental impact of the component can be expressed by Equation (29).

$$Y^{LCA}{}_k = Y^{co}{}_k + Y^{om}{}_k + Y^{de}{}_k \tag{29}$$

where $Y^{co}{}_k$, $Y^{om}{}_k$ and $Y^{de}{}_k$ are the environmental impacts of the components in the construction phase, operation and maintenance phase, and decommissioning phase.

There is a corresponding environmental impact for the working fluid that is calculated by Equation (30).

$$Y_{wf} = Y^{co}{}_{wf} + Y^{om}{}_{wf} + Y^{de}{}_{wf} \tag{30}$$

where, the environmental impact of the organic fluid is composed of the construction phase, operation and maintenance, and decomposition in mPts. However, the environmental impact of the working fluid associated with the component under study is the subject of interest. Therefore, the exergo-environmental impact is calculated, as shown in Equation (31)

$$Y^{wf}{}_k = Y_{wf} \cdot Y^*_{D,k} \quad (31)$$

where $Y^*_{D,k}$ is the exergy destruction rate of the $k$th-component.

Thus, the total environmental impact produced by the $k$th component is calculated as

$$Y^{Tot}_k = Y^{LCA}{}_k + Y^{wf}{}_k \quad (32)$$

*2.6. Exergo-Environmental Analysis*

The exergo-environmental analysis for each component is calculated according to the literature [1]. The equation for the balance of exergo-environmental impact is described by Equation (33).

$$\sum \dot{B}_{out} = \sum \dot{B}_{in} + \dot{Y}^{Tot}{}_k \quad (33)$$

where $\dot{B}$ is defined as:

$$\dot{B} = b \cdot \dot{E} \quad (34)$$

where $b$ is the specific environmental impact (mPts/GJ), $\dot{E}$ is the exergy flow (kW), and $\dot{Y}^{Tot}{}_k$ is the total environmental impact ratio of the $k$th component (mPts/h). The most relevant parameters for environmental exergy are the specific products' and inputs' environmental impacts, as described below in Equations (35) and (36).

$$b_{P,k} = \frac{\dot{B}_{P,k}}{\dot{E}_{P,k}} \quad (35)$$

$$b_{F,k} = \frac{\dot{B}_{F,k}}{\dot{E}_{F,k}} \quad (36)$$

These parameters are essential to calculate the environmental impact of the destroyed exergy, as shown in Equation (37).

$$B_{D,k} = b_{F,k} \cdot \dot{E}_{D,k} \quad (37)$$

The exergo-environmental impact of $k$th component is equal to the sum of the environmental impact caused by the destroyed manufacturing $Y_k$ and exergy, defined in Equation (38).

$$\dot{B}_k = \dot{Y}_k + \dot{B}_{D,k} \quad (38)$$

Then, having found the parameters above, the relative difference of specific environmental impact can be calculated for the $k$th component, as shown in Equation (39).

$$r_{b,k} = \frac{b_{P,k} - b_{F,k}}{\dot{b}_{P,k}} \quad (39)$$

The exergo-environmental variable $r_{b,k}$ is an indicator that reflects the component's capacity to reduce its environmental impact. When the value of $r_b$, is small, the elimination of the environmental impact of the portion in question is less important. Similarly, the exergo-environmental factor of $k$th component can be calculated, as shown in Equation (40).

$$f_{b,k} = \frac{\dot{Y}_k}{\dot{Y}_k + \dot{B}_{D,k}} = \frac{\dot{Y}_k}{\dot{B}_{D,k}} \quad (40)$$

where the exergo-environmental factor $f_{b,k}$ denotes the relation between the component's contribution to the environmental impact $\dot{Y}_k$, and the sum of the component k associated environmental impacts.

### 2.7. Advanced Exergo-Environmental Analysis

The advanced exergetic analysis is based on the separation of the environmental impacts found in each component by using the disaggregation of exergy into the endogenous, exogenous, avoidable, and unavoidable parts and the division of the same, which is composed of the endogenous avoidable/unavoidable and exogenous avoidable/unavoidable parts. This breakdown of environmental impacts is shown in Table 5.

**Table 5.** Equations related to advanced exergo-environmental analysis.

| | |
|---|---|
| Endogenous exergy destruction rate<br>$\dot{B}_{D,k}^{EN} = b_{F,k} \cdot \dot{E}_{D,k}^{EN}$ | (41) |
| Exogenous energy destruction rate<br>$\dot{B}_{D,k}^{EX} = b_{F,k} \cdot \dot{E}_{D,k}^{EX}$ | (42) |
| Avoidable exergy destruction rate<br>$\dot{B}_{D,k}^{AV} = b_{F,k} \cdot \dot{E}_{D,k}^{AV}$ | (43) |
| Unavoidable exergy destruction rate<br>$\dot{B}_{D,k}^{UN} = b_{F,k} \cdot \dot{E}_{D,k}^{UN}$ | (44) |
| Avoidable endogenous exergy destruction rate<br>$\dot{B}_{D,k}^{EN,AV} = b_{F,k} \cdot \dot{E}_{D,k}^{EN,AV}$ | (45) |
| Unavoidable endogenous exergy destruction rate<br>$\dot{B}_{D,k}^{EN,UN} = b_{F,k} \cdot \dot{E}_{D,k}^{EN,UN}$ | (46) |
| Avoidable exogenous energy destruction rate<br>$\dot{B}_{D,k}^{EX,AV} = b_{F,k} \cdot \dot{E}_{D,k}^{EX,AV}$ | (47) |
| Unavoidable exogenous energy destruction rate<br>$\dot{B}_{D,k}^{EX,UN} = b_{F,k} \cdot \dot{E}_{D,k}^{EX,UN}$ | (48) |

The $\dot{B}_{D,k}^{EN}$ is the environmental impact of the rate of exergy destroyed associated with the own irreversibilities found in the component, and $\dot{B}_{D,k}^{EX}$ is the environmental impact of the rate of exergy destroyed related to the relationship and interactions between components. Similar to the advanced exergetic analysis is the part of the environmental impacts that can be reduced $\dot{B}_{D,k}^{AV}$ through technological improvements, such as those that do not $\dot{B}_{D,k}^{UN}$. The endogenous and exogenous parts of the environmental impact associated with the exergy destruction rate will have a part that can be improved either by modifications or improvements made to the own component $\dot{B}_{D,k}^{EN,AV}$ as well as the environmental impacts that cannot be reduced in component $\dot{B}_{D,k}^{EN,UN}$, not to mention the environmental impacts that can be reduced by improvements in the other components $\dot{B}_{D,k}^{EX,AV}$, as the part which cannot be reduced $\dot{B}_{D,k}^{EX,UN}$.

## 3. Results and Discussion

### 3.1. Exergetic Analysis

For the results of the exergetic analysis, a usual engine operating condition was selected, which is described in Table 6.

**Table 6.** Main conditions for the simulation [62].

| Parameters | Values | Unit |
|---|---|---|
| Ambient temperature ($T_o$) | 30 | °C |
| Ambient pressure ($P_o$) | 101.3 | kPa |
| Turbine isentropic efficiency ($\eta_{turb}$) | 80 | % |
| Pump isentropic efficiency ($\eta_{pum}$) | 75 | % |
| Cooling water temperature ($T_{S10}$) | 50 | °C |
| Pinch point on the evaporator ($PP_{evap}$) | 15 | °C |
| Pinch point on the condenser ($PP_{cond}$) | 15 | °C |
| Minimum temperature differences ($\Delta T_{min,evap}$) | 30 | °C |
| Exhaust gas temperature ($T_{S1}$) | 435.07 | °C |
| Exhaust gas outlet temperature ($T_{S2}$) | 270 | °C |
| Pressure ratio pump-1 (rp1) | 2.5 | - |
| Pressure ratio pump-2 (rp2) | 30 | - |
| Exhaust gases mass flow ($\dot{m}_f$) | 9986.04 | kg/h |

From the simulations performed, the thermodynamic properties of each current flow were found and are shown in Table 7.

**Table 7.** Thermodynamic properties for each system flow.

| Steam | Mass Flow [kg/s] | Pressure [kPa] | Temperature [°C] | Enthalpy [kJ/kg] | Entropy [kJ/kg-K] | Exergy [kW] |
|---|---|---|---|---|---|---|
| S1 | 2.77 | 102.30 | 435.00 | −1960.43 | 0.90 | 541.10 |
| S2 | 2.77 | 101.30 | 270.00 | −2143.67 | 0.59 | 296.45 |
| S3 | 1.64 | 101.43 | 308.84 | 463.93 | 0.95 * | 209.33 |
| S3g | 1.64 | 91.45 | 271.01 | 378.65 | 0.82 * | 143.44 |
| S3f | 1.64 | 81.08 | 204.20 | 235.76 | 0.57 * | 53.32 |
| S4 | 1.64 | 68.15 | 143.72 | 116.00 | 0.32 * | 6.11 |
| S5 | 1.64 | 170.38 | 143.84 | 116.23 | 0.32 * | 6.16 |
| S6 | 0.70 | 675.85 | 278.84 | 645.65 | 1.39 | 170.24 |
| S7 | 0.70 | 22.53 | 208.40 | 524.51 | 1.45 | 71.36 |
| S7g | 0.70 | 22.53 | 65.00 | 301.64 | 0.91 | 30.64 |
| S8 | 0.70 | 22.53 | 65.00 | −87.53 | −0.24 | 2.31 |
| S9 | 0.70 | 675.85 | 65.31 | −86.47 | −0.24 | 2.88 |
| S9f | 0.70 | 675.85 | 194.20 | 181.72 | 0.43 | 49.30 |
| S9g | 0.70 | 675.85 | 194.20 | 477.95 | 1.06 | 122.52 |
| S10 | 13.09 | 101.30 | 50.00 | 209.42 | 0.70 | 34.59 |
| S10g | 13.09 | 101.30 | 55.00 | 230.33 | 0.77 | 53.50 |
| S11 | 13.09 | 101.30 | 57.86 | 242.30 | 0.79 | 66.07 |

* Entropy for the thermal oil was calculated as $s = C_p \cdot log(T/T_0)$

Table 8 shows the main results obtained from traditional exergetic analysis in detail under the condition mentioned above.

**Table 8.** Main results of the exergetic analysis for each component.

| Components | $E_F$ [kW] | $E_P$ [kW] | $E_d$ [kW] | $E_L$ [kW] | $\varepsilon_k$ [%] | $Y_{D,k}$ [%] |
|---|---|---|---|---|---|---|
| ITC 1 | 541.20 | 202.79 | 41.95 | 338.41 | 37.47 | 32.55 |
| Pump-1 | 0.37 | 0.06 | 0.31 | - | 15.61 | 0.24 |
| Turbine | 99.48 | 85.59 | 13.89 | - | 86.04 | 10.77 |
| Pump-2 | 0.76 | 0.59 | 0.17 | - | 77.60 | 0.13 |
| Evaporator | 202.85 | 166.34 | 36.51 | - | 82.00 | 28.32 |
| Condenser | - | - | 36.06 | 66.59 | - | 27.97 |

From the results obtained through the traditional exergetic analysis, it is noted that those components with the highest values of exergy destroyed should be analyzed with priority [63]; that is, the heat exchanger 1 is the component with the highest exergy destroyed with 41.95 kW (32.53%), followed by the evaporator with a value of 36.51 kW (28.326%) and the condenser very close with 36.06 kW (27.974%), the turbine with destroyed exergy of 13.89 kW (10.776%); finally, with a percentage lower than 1%, we have pump-2 and pump-1. Unfortunately, the traditional exergetic analysis does not allow to evaluate, identify, and quantify the amount of destroyed exergy produced by the component's own action and the interaction with the other components in the same measure. Therefore, an advanced exergetic analysis must be performed in order to detail and find the real potential for improvement of each component.

Figure 5 shows the variation of the thermal and exergetic efficiency, as well as the overall net system power and overall irreversibility, as a function of evaporating pressure. These results show that the increase in the vaporization pressure favors the system's efficiency. Additionally, it is observed that the destroyed exergy decreases as the evaporation pressure increases. The toluene is an alkane cycle with relatively high evaporation pressures, which favors better temperature-matching with the heat source [64]. This results in a reduction of internal heat transfer losses. That is, the entropy generation, which is the main cause of irreversibilities associated with the temperature difference between heat sources, is reduced by the increase in evaporation pressure, increasing the exergetic efficiency of the system.

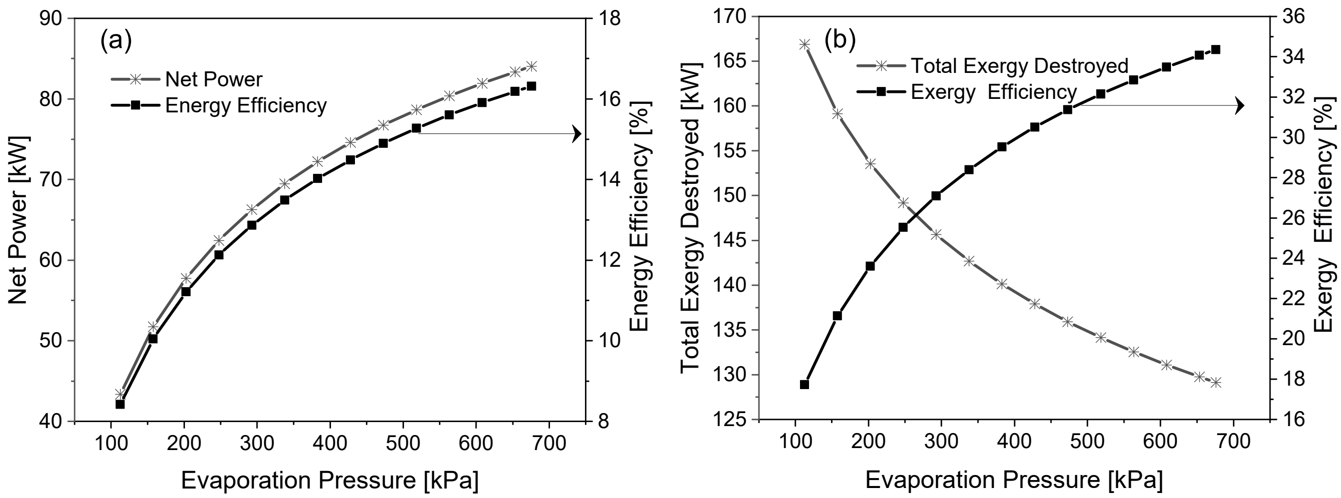


**Figure 5.** Effect of evaporation pressure on (**a**) net power and energy efficiency, (**b**) destroyed exergy and exergy efficiency.

### 3.2. Advanced Exergetic Analysis

For the calculation of the advanced exergy destroyed, the endogenous exergy of each component must first be found, so for the case study, four operating conditions were evaluated for each of the components, as shown in Table 9.

Different values of exergy destroyed were found through the simulations performed for each of the component. The intersection of the slope with respect to the *y*-axis results in the endogenous exergy destroyed. Figure 6 shows the endogenous value of each component analyzed.

The exogenous exergy destroyed was calculated by Equation (18), whose values were reported in Table 10.

For the development of the endogenous curve in the components, an unavoidable operating condition was selected in which the lowest values of exergy destroyed were given priority over the highest technological limits permissible in each component. Then, variations were made in the exergetic efficiency of the components in order to plot the endogenous curve and to find the unavoidable part, as shown in Figure 7. The unavoidable conditions of study are shown in Table 1, as well as the real and ideal conditions.

**Table 9.** Changes to the parameters chosen for each component.

| Turbine (T1) | Case 1 | Case 2 | Case 3 | Case 4 |
|---|---|---|---|---|
| rp | 30 | 60 | 90 | 120 |
| Tcond [°C] | 75 | 68 | 71 | 74 |
| $PP_{Evap}$ [°C] | 35 | 30 | 27 | 24 |
| **Pump-2 (P2)** | **Case 1** | **Case 2** | **Case 3** | **Case 4** |
| rp | 30 | 60 | 90 | 120 |
| Tcond [°C] | 71.7 | 68 | 71 | 74 |
| $PP_{Evap}$ [°C] | 32.6 | 30 | 26 | 22 |
| **Evaporator** | **Case 1** | **Case 2** | **Case 3** | **Case 4** |
| rp | 30 | 60 | 90 | 120 |
| Tcond [°C] | 70 | 68 | 71 | 74 |
| $PP_{Evap}$ [°C] | 35 | 30 | 27 | 24 |
| **Condenser** | **Case 1** | **Case 2** | **Case 3** | **Case 4** |
| rp | 30 | 60 | 90 | 120 |
| Tcond [°C] | 70 | 68 | 71 | 74 |
| $PP_{Evap}$ [°C] | 35 | 30 | 27 | 24 |
| **Pump-1 (P1)** | **Case 1** | **Case 2** | **Case 3** | **Case 4** |
| rp | 30 | 60 | 90 | 120 |
| Tcond [°C] | 71 | 68 | 71 | 74 |
| $PP_{Evap}$ [°C] | 33 | 30 | 27 | 24 |

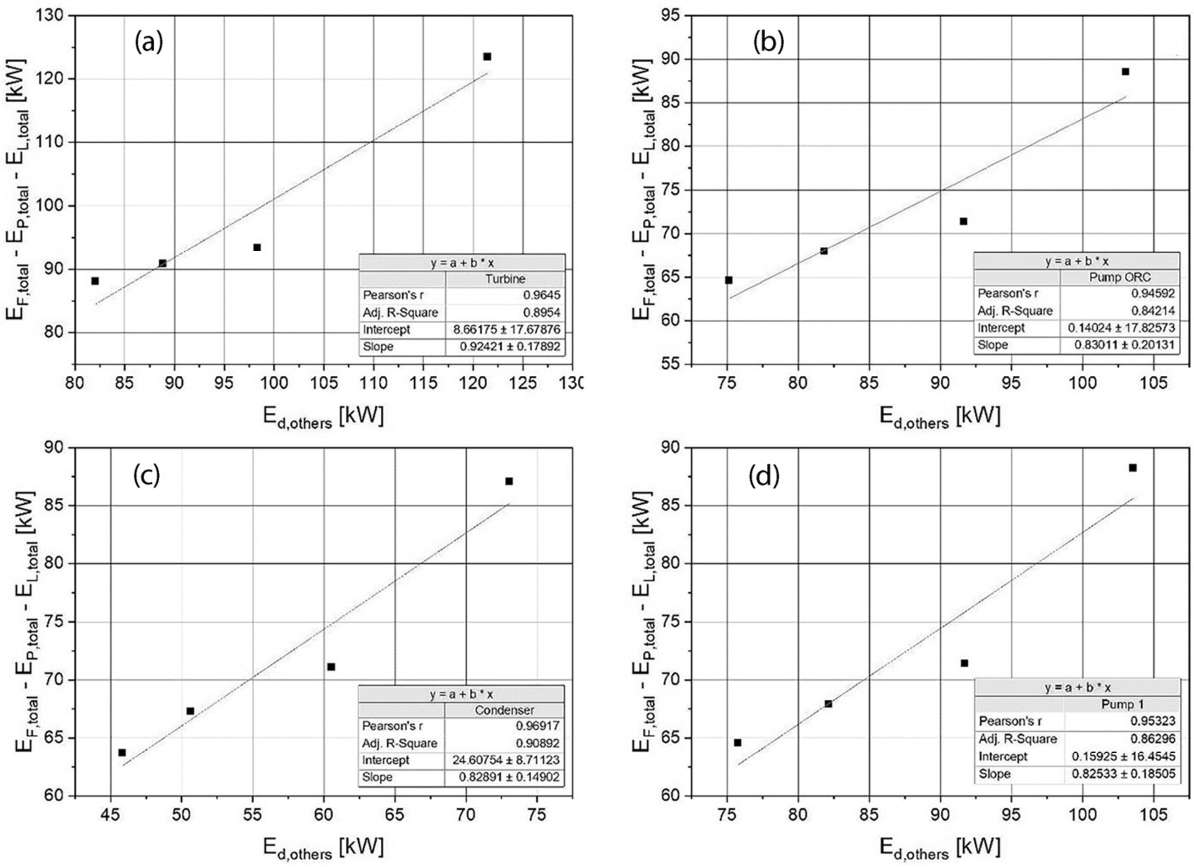


**Figure 6.** Endogenous exergy of the main components (**a**) turbine, (**b**) pump-2, (**c**) condenser, and (**d**) pump-1.

**Table 10.** Endogenous and exogenous exergy of each component destroyed.

| Components | $E_{D,k}$[kW] | $E_{D,k}^{EN}$[kW] | $E_{D,k}^{EX}$[kW] |
|---|---|---|---|
| ITC 1 | - | 41.95 | - |
| Pump-1 | 0.31 | 0.27 | 0.04 |
| Turbine | 13.89 | 8.66 | 5.23 |
| Pump-2 | 0.17 | 0.14 | 0.03 |
| Evaporator | 36.51 | 26.85 | 9.66 |
| Condenser | 36.06 | 24.61 | 11.45 |

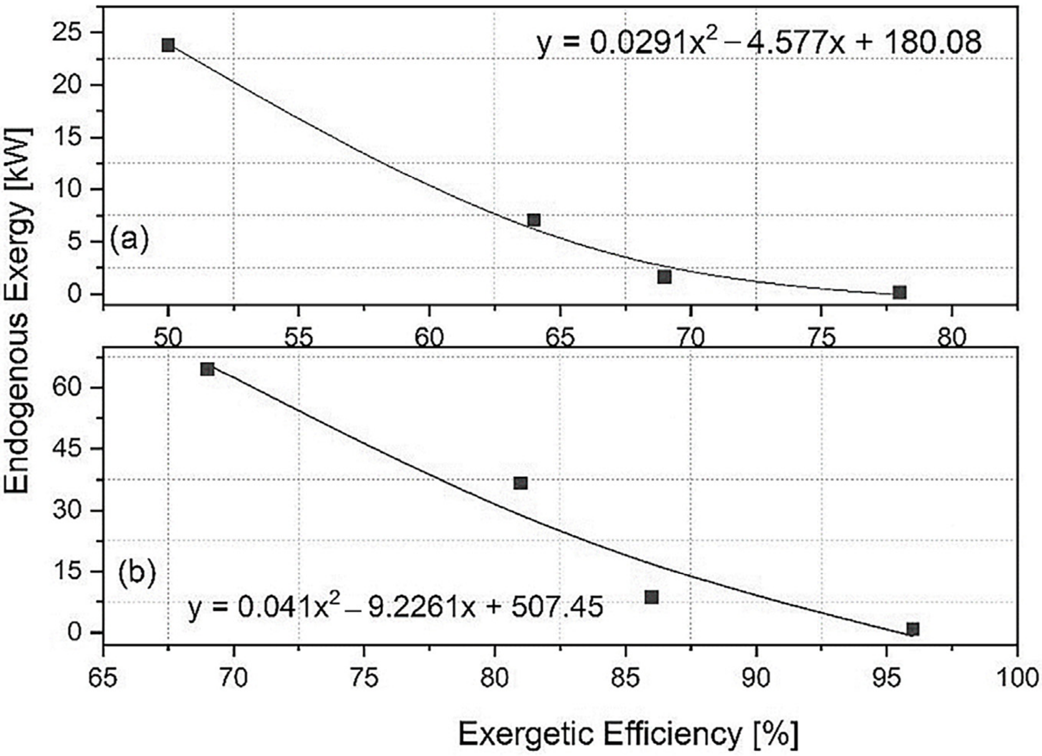


**Figure 7.** Endogenous curve (**a**) pump-2, and (**b**) turbine.

For the case of the turbine, the unavoidable endogenous exergy destruction was estimated at 0.95 kW for an exergetic efficiency of 95%. Similarly, for pump-2 it was found that the lowest value of unavoidable endogenous exergy destroyed was 0.012 kW for an exergetic efficiency of 79.05%. Using the endogenous curve, the unavoidable endogenous exergy destroyed for the turbine and pump-2 was calculated. For the heat exchanger (ITC1), evaporator, condenser, and pump-1, the value was found by using equations. Then, using Equation (16), the avoidable endogenous part was found. The disaggregation of exergy was calculated by using Equations (11)–(19) and is illustrated graphically, as shown in Figure 8.

As shown in Figure 8, in the vast majority of the components, the avoidable part is of endogenous nature so that there are opportunities for very significant improvements at the technological level in components such as the turbine, pump-1, the heat exchanger, with pump-1 as the component with the greatest opportunity for improvement of its own work (78.73%), and the turbine the component with the greatest opportunity for improvement in relation to the work carried out with the other components (12.12%). On the other hand, it is found that, for the evaporator, more than half of the exergy destroyed is of an unavoidable nature produced by the interaction that this component has in relation to the others (50.73%). The results obtained from the advanced exergetic analysis in the waste heat recovery system are detailed in Table 11.

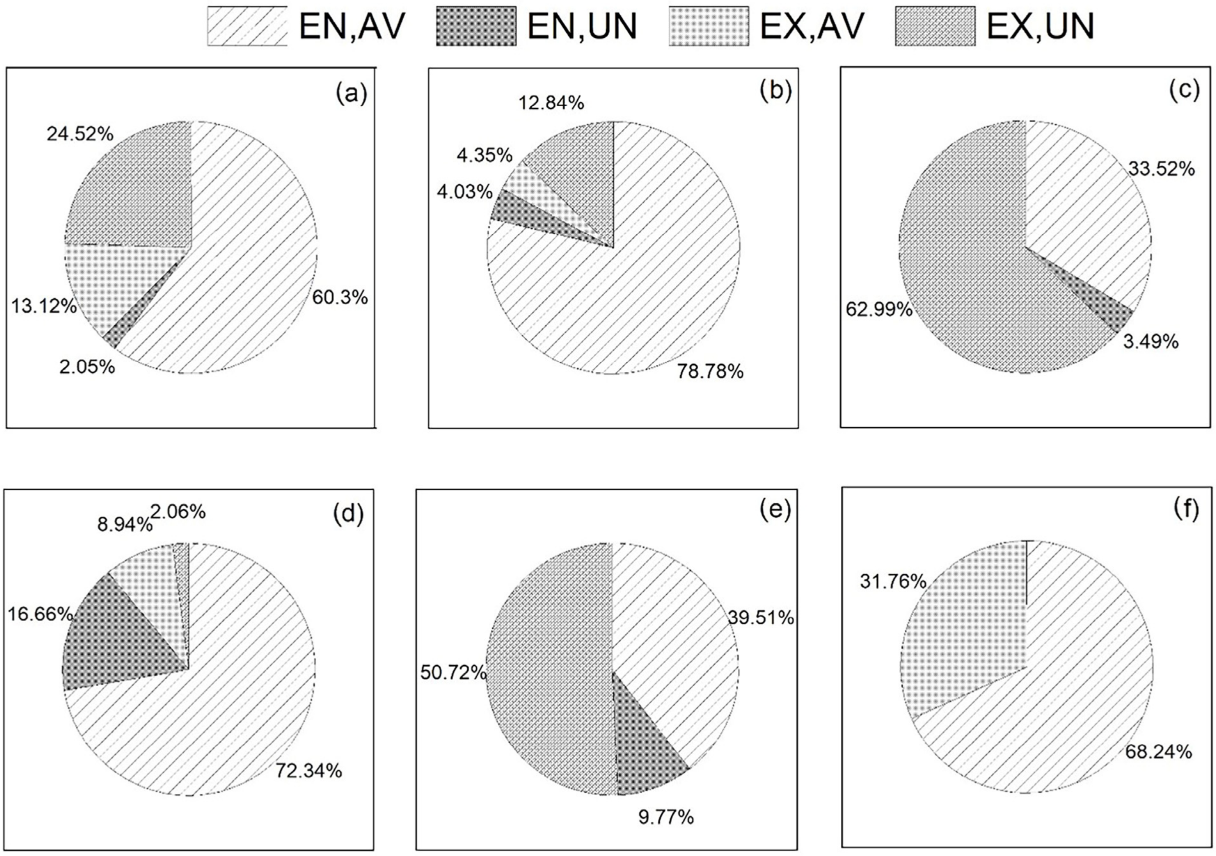


**Figure 8.** Exergy disaggregation destroyed (**a**) turbine, (**b**) pump-1, (**c**) pump-2, (**d**) ITC 1, (**e**) evaporator, and (**f**) condenser.

**Table 11.** Disaggregation of exergy destroyed for each component.

| Components | $E_{D,k}^{EN}$[kW] | $E_{D,k}^{EX}$[kW] | $E_{D,k}^{AV}$[kW] | $E_{D,k}^{UN}$[kW] | $E_{D,k}^{EN,UN}$[kW] | $E_{D,k}^{EX,UN}$[kW] | $E_{D,k}^{EN,AV}$[kW] | $E_{D,k}^{EX,AV}$[kW] |
|---|---|---|---|---|---|---|---|---|
| ITC 1 | 37.34 | 4.61 | 34.11 | 7.85 | 6.99 | 0.86 | 30.36 | 3.75 |
| Pump 1 | 0.16 | 0.16 | 0.03 | 0.03 | 0.01 | 0.27 | 0.14 | −0.11 |
| Turbine | 8.66 | 5.23 | 10.12 | 3.69 | 0.28 | 3.40 | 8.38 | 1.82 |
| Pump-2 | 0.14 | 0.03 | 0.14 | 0.03 | 0.01 | 0.02 | 0.13 | 0.01 |
| Evaporator | 26.85 | 9.66 | 3.55 | 32.97 | 5.32 | 27.64 | 21.53 | −17.98 |
| Condenser | 24.61 | 11.45 | 0.000 | 0.000 | 0.000 | 0.000 | 0.000 | 0.000 |
| Total | 97.75 | 31.14 | 48.03 | 44.57 | 12.62 | 32.21 | 60.54 | −12.41 |
| % | 75.83% | 24.16% | - | - | | | | |

From Table 11, it can be seen that interactions between components can be both positive and negative. The negative values in the exogenous destroyed exergy are mainly caused by the difference in the mass flow that occurs between the unavoidable and the ideal condition of operation, which represents variations in the thermodynamic properties of certain flows, and by high heat transfers under the same conditions, which leads to the addition of irreversibilities. When the component is studied under ideal conditions, the operating pressure of any endogenous exergy destruction is lower in the case of pump-1, due to the low efficiency of the component and the unavoidable behavior of the other components of the cycle, generating this exogenous exergy destruction condition, which is associated to similar behaviors exposed in the literature [26,35].

### 3.3. Life Cycle Assessment and Exergo-Environmental Analysis

For the shell and tube, and plate heat exchanger, a thickness of 0.002 m was chosen. A summary of the results found for each component so far is shown in Table 12 as follows.

**Table 12.** Power, heat transfer area, and exergy destroyed of each component.

| Parameters | ITC 1 | Pump-1 | Turbine | Pump-2 | Evaporator | Condenser |
|---|---|---|---|---|---|---|
| W [kW] | - | 0.37 | 85.59 | 0.76 | - | - |
| Q [kW] | 514.85 | - | - | - | 515.23 | 430.39 |
| A [$m^2$] | 88.70 | - | - | - | 27.61 | 14.32 |
| $E_{D,k}$ [kW] | 41.95 | 0.31 | 13.89 | 0.17 | 36.51 | 13.06 |

With the data obtained so far, and by applying Equations (25)–(30), a summary of the environmental properties and impacts that were calculated on each of the components when steel for construction was chosen, the thermal oil was diphenyl oxide, and the working fluid was toluene. The eco-99 coefficient ($\varphi_k$) for the steel materials was 86 mPts/kg, for the thermal was 46,467 mPts/kg, and for the organic fluid was 2634 mPts/kg [34]. The environmental impact in mPts and the amount of material by component are shown in Figure 9.

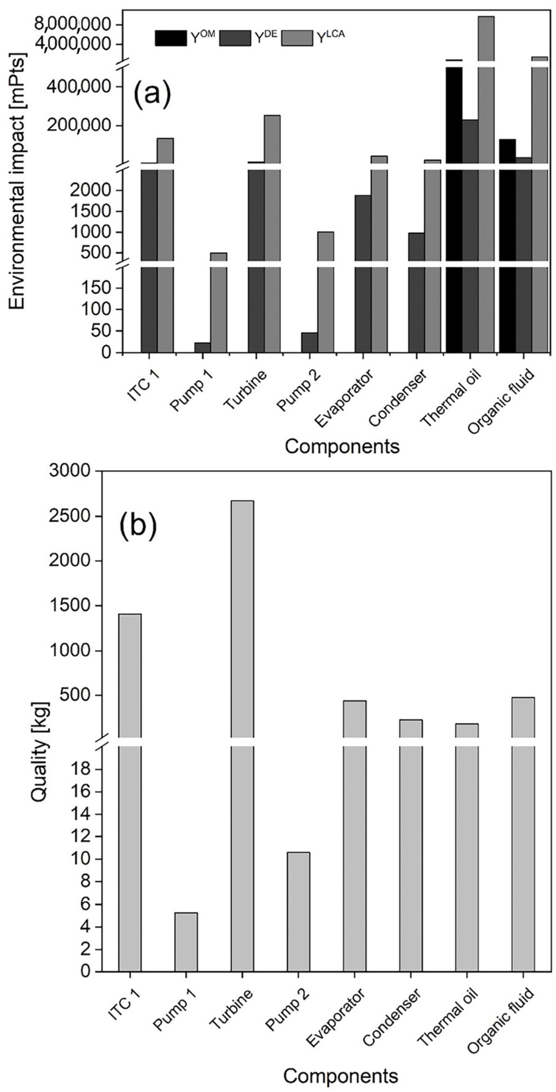


**Figure 9.** Life cycle analysis results for steel for (**a**) Environmental impact and, (**b**) Quality.

Table 13 shows the total environmental impact in mPts/h associated with each component when taking into account the organic fluid during the whole life of the plant, which is a total of 7446 h per year for 20 years.

**Table 13.** Total environmental impacts for each component over its lifetime.

| Parameters | ITC 1 | Pump-1 | Turbine | Pump-2 | Evaporator | Condenser |
|---|---|---|---|---|---|---|
| $Y_k^{wf}$ [mPts] | 90,119.94 | 679.31 | 29,838.73 | 363.80 | 78,432.35 | 77,456.15 |
| $Y_k^{LCA}$ [mPts] | 133,081.57 | 496.29 | 252,782.47 | 1001.50 | 41,428.33 | 21,481.49 |
| $Y_k^{Tot}$ [mPts] | 223,201.51 | 1175.60 | 282,621.20 | 1365.30 | 119,860.69 | 98,937.64 |
| $\dot{Y}_k^{Tot}$ [mPts/h] | 0.89 | 0.003 | 1.69 | 0.007 | 0.28 | 0.14 |

The equations for the traditional exergetic part were necessary to find the environmental impacts per unit of exergy of input, output, and losses in each component. The values recorded are tabulated in Table 14.

A comparison between the values found in Section 3.1, and the environmental impacts associated with product exergy, fuel, and loss, infers that there is little relationship between them. For example, in the case of the ITC1, which was the component with the highest irreversibility, it was found that it only has the highest environmental impact in terms of exergy of losses caused by the high temperature of the exhaust gases at the outlet of the same component. Generally speaking, the component with one of the greatest environmental impacts is the condenser, being the component with the greatest environmental impact associated with the concept of fuel and destroyed exergy. In other words, in those components in which heat is exchanged, the environmental impacts per unit of exergy are greater, unlike the turbine and pump, which are the least contaminating components.

For the conditions previously analyzed, it is possible to know in which of all the components there are greater opportunities for improvement in terms of the reduction of the environmental impacts generated by evaluating the parameter $r_{b,k}$. For the case of study, it is observed that pump-1 and the condenser are the components that have a higher environmental ratio with 579.15% and 116.78%, respectively, showing that their environmental impacts can be reduced more easily, contrary to components such as the evaporator and heat exchanger 1, which have the lowest values of the environmental ratio $r_{b,k}$.

**Table 14.** Traditional exergo-environmental parameters for each component.

| Components | $b_F$ [mPts/MJ] | $b_P$ [mPts/MJ] | $\dot{B}_L$ [mPts/h] | $\dot{B}_D$ [mPts/h] | $r_{b,k}$ [%] | $f_{b,k}$ [%] |
|---|---|---|---|---|---|---|
| ITC 1 | 0.04 | 0.02 | 45.79 | 6.48 | 23.54 | 12.12 |
| Pump-1 | 0.04 | 0.28 | - | 0.05 | 579.15 | 6.64 |
| Turbine | 0.03 | 0.04 | - | 1.53 | 34.17 | 52.51 |
| Pump-2 | 0.04 | 0.05 | - | 0.02 | 36.59 | 21.12 |
| Evaporator | 0.02 | 0.03 | - | 3.25 | 23.83 | 7.89 |
| Condenser | 0.07 | 0.03 | 16.12 | 8.73 | 116.78 | 1.63 |

Similarly, it can be seen that the component with the greatest environmental impact due to the manufacturing process is the turbine, obtaining the highest value of exergo-environmental fraction with 52.51%, followed by pump-2 with 21.12%. It can be observed that for this particular case, the components with the highest value $r_{b,k}$ have the lowest values of $f_{b,k}$, so that the attention to these components should be focused on the generation of environmental impacts in relation to their exergy $\dot{B}_k$.

### 3.4. Advanced Exergo-Environmental Analysis

In order to enrich the knowledge, the same methodology was applied for the advanced exergetic analysis to find opportunities for environmental improvements in the components, where a comparison between the components was made, as shown in Table 15.

**Table 15.** Associated environmental impact by exergy on each component.

| Components | $\dot{B}_{D,k}^{EN}$ [mPts/h] | $\dot{B}_{D,k}^{EX}$ [mPts/h] | $\dot{B}_{D,k}^{AV}$ [mPts/h] | $\dot{B}_{D,k}^{UN}$ [mPts/h] | $\dot{B}_{D,k}^{EN,UN}$ [mPts/h] | $\dot{B}_{D,k}^{EX,UN}$ [mPts/h] | $\dot{B}_{D,k}^{EN,AV}$ [mPts/h] | $\dot{B}_{D,k}^{EX,AV}$ [mPts/h] |
|---|---|---|---|---|---|---|---|---|
| ITC 1 | 5.77 | 0.71 | 5.27 | 1.21 | 1.08 | 0.13 | 4.69 | 0.58 |
| Pump-1 | 0.02 | 0.02 | 0.004 | 0.004 | 0.002 | 0.04 | 0.02 | −0.02 |
| Turbine | 0.96 | 0.58 | 1.13 | 0.41 | 0.03 | 0.38 | 0.92 | 0.20 |
| Pump-2 | 0.02 | 0.004 | 0.02 | 0.004 | 0.001 | 0.003 | 0.02 | 0.001 |
| Evaporator | 2.39 | 0.86 | 0.32 | 2.93 | 0.47 | 2.46 | 1.91 | −1.60 |
| Condenser | 5.96 | 2.77 | 0.00 | 0.00 | 0.00 | 0.00 | 0.00 | 0.00 |

From Table 15, it can be seen that the components that generate the greatest environmental impacts by their very nature are those components in which heat is exchanged, the first of these being in the condenser producing an endogenous environmental impact of 5.96 mPts/h (39.4%), followed by the ITC1 with 5.77 mPts/h (38.16%), and closing with the evaporator with a value of 2.39 (15.8%). Other components such as the turbine and the pumps make up the minority with 6.33% for the turbine and a representative value of less than 1% for the pumps, respectively. For all the components, it was found that the environmental impacts are mostly associated with the operating conditions of the component itself, so that there were very low values in the exogenous environmental impact for the whole system.

### 3.5. Sensitivity Analysis

The life cycle analysis of the waste heat recovery system was carried out using copper and aluminum as material in order to find the environmental impacts generated by the components by the construction materials. Table 16 shows the total environmental impact associated with each component when the materials are taken into account.

**Table 16.** Life cycle analysis results for copper and aluminum.

| Material | Components | w [mPts/kg] | Quality [kg] | $Y^{co}$ [mPts] | $Y^{om}$ [mPts] | $Y^{de}$ [mPts] | Y [mPts] |
|---|---|---|---|---|---|---|---|
| Copper | ITC 1 | 1400 | 1589.50 | 2,336,570.88 | 0 | 111,265.28 | 2,447,836.16 |
| | Pump-1 | 1400 | 5.89 | 8653.84 | 0 | 412.09 | 9065.93 |
| | Turbine | 1400 | 2998.22 | 4,407,379.03 | 0 | 209,875.19 | 4,617,254.22 |
| | Pump-2 | 1400 | 11.88 | 17,463.30 | 0 | 831.59 | 18,294.88 |
| | Evaporator | 1400 | 494.82 | 727,386.38 | 0 | 34,637.45 | 762,023.82 |
| | Condenser | 1400 | 2565.71 | 3,771,598.40 | 0 | 179,599.92 | 3,951,198.33 |
| | Thermal oil | 46,467 | 184.00 | 8,568,514.8 | 856,851.48 | 231,349.90 | 9,656,716.18 |
| | Organic fluid | 2679.8 | 476.74 | 1,277,557.65 | 127,755.76 | 34,494.05 | 1,439,807.47 |
| Aluminum | ITC 1 | 780 | 478.67 | 392,052.15 | 0 | 18,669.15 | 410,721.30 |
| | Pump-1 | 780 | 5.58 | 4573.80 | 0 | 217.80 | 4791.60 |
| | Turbine | 780 | 2844.35 | 2,329,523.03 | 0 | 110,929.67 | 2,440,452.70 |
| | Pump-2 | 780 | 11.27 | 9229.85 | 0 | 439.52 | 9669.37 |
| | Evaporator | 780 | 149.02 | 122,047.83 | 0 | 5811.80 | 127,859.62 |
| | Condenser | 780 | 772.69 | 632,834.76 | 0 | 30,134.99 | 662,969.75 |
| | Thermal oil | 46,467 | 184.00 | 8,568,514.8 | 856,851.48 | 231,349.89 | 9,656,716.18 |
| | Organic fluid | 2679.8 | 476.73 | 1,277,557.65 | 127,755.76 | 34,494.05 | 1,439,807.47 |

The division of exergy destruction into endogenous/exogenous and avoidable/unavoidable components of the cycle for the development of advanced exergo-environmental analysis was made in Section 3.4, which will be used in the evaluation of environmental impacts for each of the components. The divisions of environmental impacts for copper are shown in Table 17.

**Table 17.** Associated environmental impact by exergy on each component using copper as a material.

| Components | $\dot{B}_{D,k}^{EN}$ [mPts/h] | $\dot{B}_{D,k}^{EX}$ [mPts/h] | $\dot{B}_{D,k}^{AV}$ [mPts/h] | $\dot{B}_{D,k}^{UN}$ [mPts/h] | $\dot{B}_{D,k}^{EN,UN}$ [mPts/h] | $\dot{B}_{D,k}^{EX,UN}$ [mPts/h] | $\dot{B}_{D,k}^{EN,AV}$ [mPts/h] | $\dot{B}_{D,k}^{EX,AV}$ [mPts/h] |
|---|---|---|---|---|---|---|---|---|
| ITC 1 | 25.09 | 3.10 | 22.92 | 5.27 | 4.69 | 0.58 | 20.40 | 2.52 |
| Pump-1 | 0.16 | 0.16 | 0.03 | 0.02 | 0.01 | 0.28 | 0.15 | −0.12 |
| Turbine | 5.04 | 3.04 | 5.94 | 2.15 | 0.16 | 1.98 | 4.88 | 1.06 |
| Pump-2 | 0.14 | 0.03 | 0.15 | 0.03 | 0.007 | 0.02 | 0.14 | 0.007 |
| Evaporator | 12.08 | 4.35 | 1.59 | 14.83 | 2.39 | 12.44 | 9.68 | −8.09 |
| Condenser | 51.59 | 24.01 | 0.00 | 0.00 | 0.00 | 0.00 | 0.00 | 0.00 |

Table 18 shows the division of environmental impacts for each component, using aluminum as the material.

**Table 18.** Associated environmental impact by exergy on each component using aluminum as a material.

| Components | $\dot{B}_{D,k}^{EN}$ [mPts/h] | $\dot{B}_{D,k}^{EX}$ [mPts/h] | $\dot{B}_{D,k}^{AV}$ [mPts/h] | $\dot{B}_{D,k}^{UN}$ [mPts/h] | $\dot{B}_{D,k}^{EN,UN}$ [mPts/h] | $\dot{B}_{D,k}^{EX,UN}$ [mPts/h] | $\dot{B}_{D,k}^{EN,AV}$ [mPts/h] | $\dot{B}_{D,k}^{EX,AV}$ [mPts/h] |
|---|---|---|---|---|---|---|---|---|
| ITC 1 | 8.69 | 1.07 | 7.94 | 1.82 | 1.62 | 0.20 | 7.06 | 0.87 |
| Pump-1 | 0.06 | 0.06 | 0.01 | 0.01 | 0.006 | 0.11 | 0.06 | −0.04 |
| Turbine | 1.55 | 0.94 | 1.82 | 0.66 | 0.05 | 0.61 | 1.50 | 0.32 |
| Pump-2 | 0.05 | 0.01 | 0.05 | 0.01 | 0.003 | 0.009 | 0.05 | 0.003 |
| Evaporator | 3.79 | 1.37 | 0.50 | 4.66 | 0.75 | 3.91 | 3.04 | −2.54 |
| Condenser | 12.97 | 6.03 | 0.00 | 0.00 | 0.00 | 0.00 | 0.00 | 0.00 |

When obtaining the data of the exergo-environmental analysis of the materials steel, copper, and aluminum, a comparative analysis was made between the analysis, taking results the environmental impact of the components changing their material as shown in Figure 10.

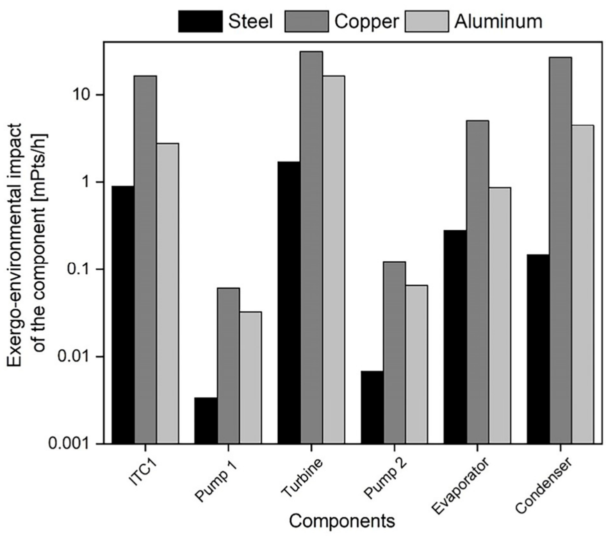


**Figure 10.** Exergo-environmental impacts of the components with respect to the materials under study.

For the copper values, the exergo-environmental impacts increased considerably for each of the heat recovery system components, reaching maximum values of 32 mPts/h in the case of the turbine, so the exergo-environmental impact of the components is mainly composed of the environmental impact of the life cycle analysis. For the values of aluminum, the exergo-environmental impacts of the components increased with respect to the steel, the component with the greatest impact being the turbine with 22 mPts/h. Contrary to the material copper, the exergo-environmental impacts of the components are mainly composed of the environmental impact of the destroyed exergy.

Taking into account the virtues evaluated in each material, steel generates the least exergo-environmental impacts with respect to the materials in the study, because according to Eco-Indicator 99, steel has a lower coefficient than copper and aluminum, so, in the mass of each component, the exergo-environmental impact of any material with steel should be less than the impacts generated using copper and aluminum.

In Figure 11, the impact of the pressure ratio (rp) on the exergo-environmental ratio rb,k was evaluated, which is an indicator that reflects the potential for reducing the environmental impact of each component, of each of the components for each of the materials using toluene as working fluid. In Figure 11a, it is evaluated taking as material the steel, in which similar behaviors are shown for the pump-1 and the evaporator, decreasing its value between values of 1%, opposite case to the condenser, pump-2 and the turbine, finding a considerable increase when increasing the value of the pressure ratio. A case not exempt to the others is presented with the heat exchanger ITC1, where when approaching values of rp = 15, a reduction of the value of $r_{b,k}$ is produced, which can be caused by the generation of inevitable exogenous energy. In Figure 11b, where copper is taken as material, the same behavior of Figure 11a is presented, where the turbine takes values of almost three times that of using a turbine taking steel as material. The ITC1 heat exchanger takes the same behavior as in Figure 11a, but the decrease in value occurs around rp = 20. In Figure 11c, the behavior of the components using aluminum as a construction material is shown, where the same behavior as in the previous graphs is replicated, but pump-1, pump-2, turbine, and ITC1 increase their $r_{b,k}$ values above the other materials for comparison. The turbine is emitted because its values are four times higher than those obtained using steel as a material.

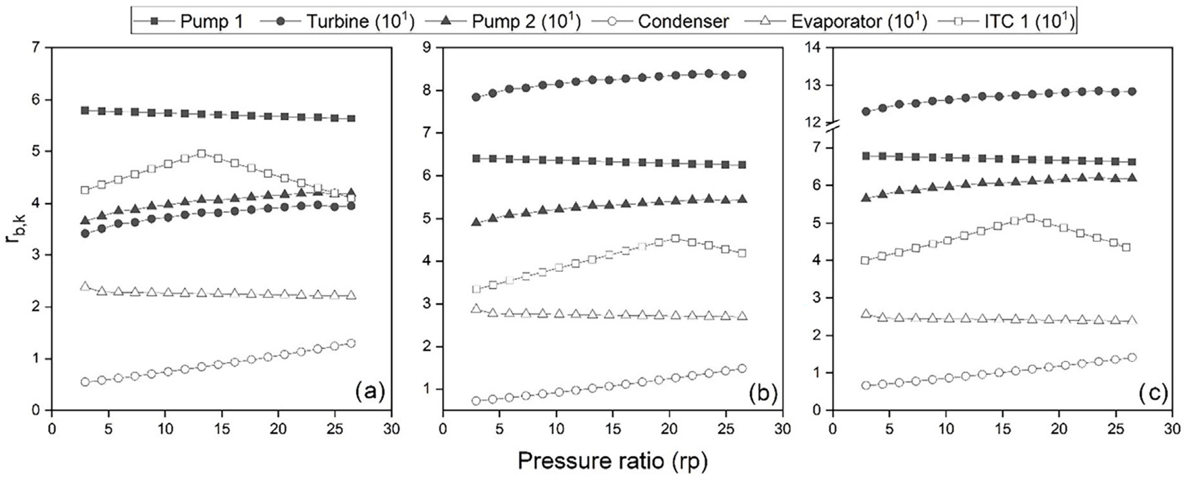


**Figure 11.** Relative difference in the specific environmental impact of the components using (**a**) steel, (**b**) copper, (**c**) aluminum as a base material.

The definition of the exergo-environmental variable $r_b$ mentions that, between a higher value of $r_{b,k}$, there is a greater potential for reduction of environmental impacts, which is reflected in the components. If the material aluminum is used, there is the possibility of reducing the greatest number of environmental impacts in the components.

Figure 12 shows the behavior of the exergo-environmental fraction applied in the WHRS for the selected materials taking as input the pressure ratio. In Figure 12a, the behavior of the exergo-environmental fraction using steel as material is shown. A linear behavior is given where the value of $f_{b,k}$ does not vary upwards much for components such as pump-1 and the condenser, and downwards for the turbine. However, cases where it is reflected with significant changes are in the heat exchanger ITC 1 and the evaporator, and the case of the pump-2, where from rp = 2.34 and rp = 26, the value of $f_{b,k}$ decreases in an exponential way, which is repeated for the materials. In Figure 12b, the behaviour of $f_{b,k}$ using copper as the component material is shown. The behavior of the material copper is similar to that of steel, with the difference that the capacitor behaves linearly and does not change much. In Figure 12c, the behavior of the exergo-environmental fraction is shown using aluminum as component material.

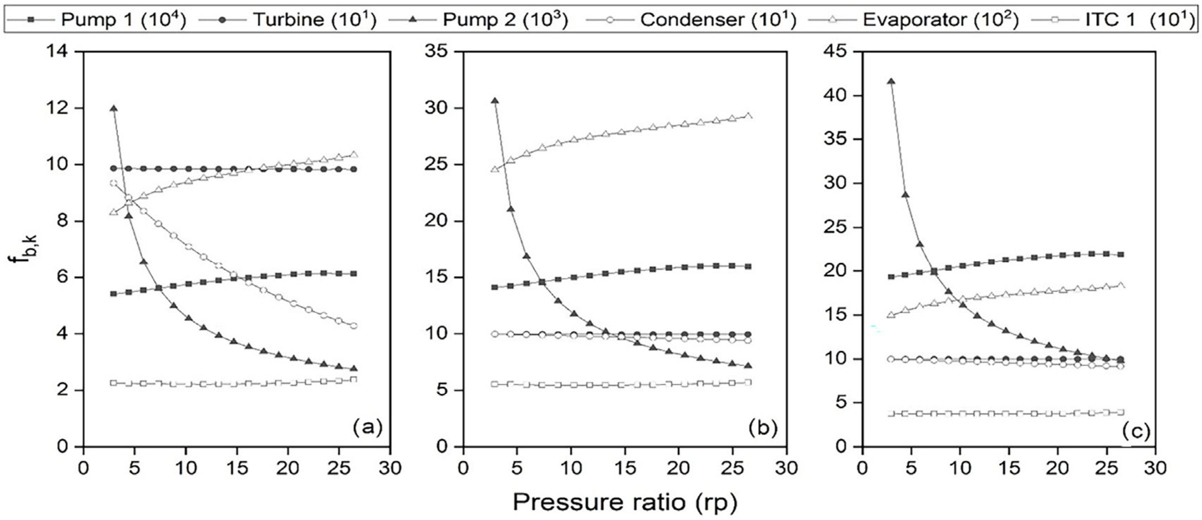


**Figure 12.** Exergo-environmental factor of the components using (**a**) steel, (**b**) copper, (**c**) aluminum as a base material.

With respect to the steel and copper materials, the components with aluminum have a high environmental fraction, following the behavior of the copper material. Pump-2 has a decreasing behavior; this must be because the impacts generated by the destruction of exergy as the rp increases are greater than the impacts generated by the manufacture of the component, generating that the value of the exergo-environmental fraction goes down considerably. The behavior of the condenser for the steel is of a decreasing manner as the rp varies ascending; on the other hand, for the copper and aluminum it has a reduction of the value of $r_{b,k}$ and it does not differ much, indicating that in the steel the impacts generated by the destruction of exergy affects more when reducing the environmental impacts.

## 4. Conclusions

The traditional and advanced exergetic analyses show that the components that must be improved in order of priority, for the traditional exergetic analysis, are the ITC1 (32.5%), evaporator (28.3%), condenser (27.9%), and turbines and pumps in the last place. On the other hand, for advanced exergetic analysis, components such as pump-1 have the maximum real potential for improvement, avoiding more than 80% of its exergy destroyed (78.77% endogenous and 4.38% exogenous), but this does not generate a great change in the performance of the entire system, as is the case with the ITC1, whose endogenous exergy destroyed is greater than 70%. As it is the component with the greatest irreversibilities, a technological improvement would increase the performance and efficiency of the ORC heat recovery cycle.

Through life cycle analysis, the environmental impact of each component could be calculated when the material chosen for these was steel. According to the results of the traditional exergo-environmental analysis, it was found that the component with the greatest environmental impact associated with exergy and per unit of exergy was the condenser (bf = 0.06 mPts/MJ and $\dot{B}D$ = 8.73 mPts/h), and the components with less environmental impact per unit of exergy were the evaporator with an environmental impact value per unit of exergy of bf = 0.02 mPts/MJ, and the pump-2 with an environmental impact assessment associated with exergy of $\dot{B}D$ = 0.025 mPts/h. In the advanced exergo-environmental analysis carried out, it was found that the environmental impact is associated to a greater extent with the behavior of the components, representing 75.33% of the environmental impacts of endogenous nature, showing that the environmental impacts are generated to a lesser extent by the interactions between components. The heat exchangers were the components that generated a greater environmental impact than the other components. However, these can be reduced by 81.3%. The sensitivity analysis was carried out with three different materials (steel, copper, and aluminum), and it was found that steel generates the lowest environmental impacts and generates high opportunities for improvement by evaluating with the exergo-environmental factor and the exergo-environmental relationship using the pressure ratio, representing the most efficient material for the selection of the components.

For future work, it is recommended that more precise analyses be carried out using data approximation techniques to obtain more accurate values of performance in this type of cycle, as well as evaluating this proposal with other organic fluids by means of conventional and advanced exergetic analyses. Similarly, it is recommended to continue evaluating the indicators studied previously, and a proposal is suggested for multivariate methods that will allow the recovery power of this type of system to be maximized at different points of operation.

**Author Contributions:** Conceptualization, A.B.G., J.C.V. and R.D.H.; methodology, A.B.G., J.C.V. and G.V.O.; software, A.B.G., J.C.V. and R.D.H.; validation, J.D.F., G.V.O. and R.D.H.; formal analysis, J.D.F. and G.V.O.; investigation, J.D.F. and G.V.O.; resources, J.D.F. and G.V.O.; writing—original draft preparation, A.B.G. and J.C.V.; writing—review and editing, J.D.F. and G.V.O.; visualization, A.B.G. and J.C.V.; supervision, J.D.F. and G.V.O. All authors have read and agreed to the published version of the manuscript.

**Funding:** This research received no external funding.

**Data Availability Statement:** Not applicable.

**Acknowledgments:** This investigation was supported by the Mechanical Engineering Program of the Universidad del Atlántico. The KAI Research Group supports A. Benavides, J. Camargo, G. Valencia, J. Duarte, and R. Diaz. In addition, the authors would like to dedicate this work to the memory of our colleague, friend, and author of this research, Aldair Benavides Gamero, who was an important part of this work and also in our lives. Rest in Peace, old friend.

**Conflicts of Interest:** The authors declare no conflict of interest.

## Abbreviations

The following abbreviations are used in this manuscript:

| | |
|---|---|
| Abbreviations | |
| ORC | Organic Rankine Cycle |
| ODP | Ozone depression potential |
| GWP | Global warming potential |
| WHRS | Waste Heat Recovery System |
| LCA | Life Cycle Assessments |
| HX1 | Heat Exchanger 1 |
| ITC | Heat Exchanger |
| LMTD | logarithmic mean temperature difference |
| Nomenclature | |
| $A$ | Area, m$^2$ |
| $b$ | Environmental impact points per unit of exergy, mPts/kJ |
| $\dot{B}$ | Environmental impact rate associated with exergy, mPts/h |

| | |
|---|---|
| $Cp$ | Specific heat, kJ/kg K |
| $D$ | Diameter, m |
| $e_k$ | Specific exergy, kJ/kg |
| $\dot{E}$ | Exergy rate, kW |
| $F_T$ | Temperature correction factor |
| $f_b$ | Exergo-environmental factor |
| $h$ | Specific enthalpy, kJ/kg |
| $M_k$ | Mass, kg |
| $\dot{m}_k$ | Mass flow, kg/s |
| $P$ | Pressure, kPa |
| $\dot{Q}$ | Heat rate, kW |
| $R$ | Universal gas constant or coefficient of effectiveness |
| $r_b$ | Relative difference of specific environmental impact, % |
| $rp$ | Pressure ratio |
| $S$ | Heat capacity ratio |
| $s$ | Specific entropy, kJ/kg · K |
| $T$ | Temperature, °C |
| $U$ | Overall heat transfer coefficient, W/m$^2$ · K |
| $u$ | Internal energy, J |
| $v$ | Volume, m$^3$ |
| $\dot{W}$ | Power, kW |
| $\dot{X}_D$ | Exergy destruction rate, kW |
| $X_i$ | Gas mole fraction |
| $Y_k$ | Environmental impact, mPts |
| $\dot{Y}_k$ | Environmental impact related to the component, mPts/h |
| $y_{D,k}$ | Exergy destruction fraction, % |
| Subscripts | |
| $wf$ | Working fluid |
| $cond$ | Condensator |
| $evap$ | Evaporator |
| $D$ | Destroyed |
| $F$ | Fuel (exergy) |
| $k$ | $k$-th component |
| $L$ | Lost (exergy) |
| $in$ | Input |
| $pum$ | Pump |
| $P$ | Product (exergy) |
| $out$ | Output |
| $VC$ | Control volume |
| $Sys$ | Sistem |
| $tur$ | Turbine |
| $tot$ | Total |
| 0 | Reference condition |
| Superscripts | |
| $EN$ | Endogenous |
| $EX$ | Exogenous |
| $AV$ | Avoidable |
| $UN$ | Unavoidable |
| $ph$ | Physical |
| $ch$ | Chemical |
| $id$ | Ideal system |
| $Rs$ | Real system |
| co | Contruction phase |
| om | Operation and maintance phase |
| de | Decommissioning phase |

Greek letters

| | |
|---|---|
| $\epsilon_k$ | Exergetic efficiency, % |
| $\varphi_k$ | Eco-99 coefficient |
| $\rho$ | Density, kg/m$^3$ |
| $\delta$ | Thickness, m |
| $\alpha$ | Mass of material per k, kg/kW |

## References


1. Meyer, L.; Tsatsaronis, G.; Buchgeister, J.; Schebek, L. Exergoenvironmental analysis for evaluation of the environmental impact of energy conversion systems. *Energy* **2009**, *34*, 75–89. [CrossRef]
2. Audenaert, A.; De Cleyn, S.H.; Buyle, M. LCA of low-energy flats using the Eco-indicator 99 method: Impact of insulation materials. *Energy Build.* **2012**, *47*, 68–73. [CrossRef]
3. Chaiyat, N.; Chaongew, S.; Ondokmai, P.; Makarkard, P. Levelized energy and exergy costings per life cycle assessment of a combined cooling, heating, power and tourism system of the San Kamphaeng hot spring, Thailand. *Renew. Energy* **2020**, *146*, 828–842. [CrossRef]
4. Heijungs, R.; Huppes, G.; Guinée, J.B. Life cycle assessment and sustainability analysis of products, materials and technologies. Toward a scientific framework for sustainability life cycle analysis. *Polym. Degrad. Stab.* **2010**, *95*, 422–428. [CrossRef]
5. Jiang, R.; Wu, P. Estimation of environmental impacts of roads through life cycle assessment: A critical review and future directions. *Transp. Res. Part D Transp. Environ.* **2019**, *77*, 148–163. [CrossRef]
6. Nwodo, M.N.; Anumba, C.J. A review of life cycle assessment of buildings using a systematic approach. *Build. Environ.* **2019**, *162*, 106290. [CrossRef]
7. Ameri, M.; Mohammadzadeh, M. Thermodynamic, thermoeconomic and life cycle assessment of a novel integrated solar combined cycle (ISCC) power plant. *Sustain. Energy Technol. Assess.* **2018**, *27*, 192–205. [CrossRef]
8. Ayres, R.U.; Ayres, L.W.; Martinás, K. Exergy, waste accounting, and life-cycle analysis. *Energy* **1998**, *23*, 355–363. [CrossRef]
9. Koroneos, C.; Tsarouhis, M. Exergy analysis and life cycle assessment of solar heating and cooling systems in the building environment. *J. Clean. Prod.* **2012**, *32*, 52–60. [CrossRef]
10. Laner, D.; Rechberger, H.; De Soete, W.; De Meester, S.; Astrup, T.F. Resource recovery from residual household waste: An application of exergy flow analysis and exergetic life cycle assessment. *Waste Manag.* **2015**, *46*, 653–667. [CrossRef]
11. Param, H.K.; Jianu, O.A. Exergy Analysis of Heat Recovery Steam Generator: Effects of Supplementary Firing and Desuperheater. *J. Energy Resour. Technol.* **2020**, *142*, 50908. [CrossRef]
12. Keçebaş, A. Exergoenvironmental analysis for a geothermal district heating system: An application. *Energy* **2016**, *94*, 391–400. [CrossRef]
13. Ahmadi, P.; Dincer, I. Exergoenvironmental analysis and optimization of a cogeneration plant system using Multimodal Genetic Algorithm (MGA). *Energy* **2010**, *35*, 5161–5172. [CrossRef]
14. Boyano, A.; Blanco-Marigorta, A.M.; Morosuk, T.; Tsatsaronis, G. Exergoenvironmental analysis of a steam methane reforming process for hydrogen production. *Energy* **2011**, *36*, 2202–2214. [CrossRef]
15. Petrakopoulou, F.; Boyano, A.; Cabrera, M.; Tsatsaronis, G. Exergoeconomic and exergoenvironmental analyses of a combined cycle power plant with chemical looping technology. *Int. J. Greenh. Gas Control* **2011**, *5*, 475–482. [CrossRef]
16. Tsatsaronis, G. *Strengths and Limitations of Exergy Analysis BT–Thermodynamic Optimization of Complex Energy Systems*; Bejan, A., Mamut, E., Eds.; Springer: Dordrecht, The Netherlands, 1999; pp. 93–100. [CrossRef]
17. Colorado-Garrido, D. Advanced Exergy Analysis of a Compression–Absorption Cascade Refrigeration System. *J. Energy Resour. Technol.* **2018**, *141*, 42002. [CrossRef]
18. Petrakopoulou, F. Comparative Evaluation of Power Plants with $CO_2$ Capture: Thermodynamic, Economic and Environmental Performance. Doctoral Thesis, Technische Universität Berlin, Berlin, Germany, 2010. [CrossRef]
19. Naeimi, M.M.; Salehi, G.R.; Yazdi, M.E. Advanced Exergy, Exergoeconomic, Exergoenvironmnetal Evaluation of a Solar Hybrid Trigeneration System based on Solar-Gas Turbine for an Office Building. *J. Energy Resour. Technol.* **2020**, *143*, 1–9. [CrossRef]
20. Boyano, A.; Morosuk, T.; Blanco-Marigorta, A.M.; Tsatsaronis, G. Conventional and advanced exergoenvironmental analysis of a steam methane reforming reactor for hydrogen production. *J. Clean. Prod.* **2012**, *20*, 152–160. [CrossRef]
21. Petrakopoulou, F.; Tsatsaronis, G.; Morosuk, T. Advanced exergoenvironmental analysis of a near-zero emission power plant with chemical looping combustion. *Environ. Sci. Technol.* **2012**, *46*, 3001–3007. [CrossRef]
22. Açıkkalp, E.; Aras, H.; Hepbasli, A. Advanced exergoenvironmental assessment of a natural gas-fired electricity generating facility. *Energy Convers. Manag.* **2014**, *81*, 112–119. [CrossRef]
23. Petrakopoulou, F.; Tsatsaronis, G.; Morosuk, T. Assessment of a Power Plant With CO2 Capture Using an Advanced Exergoenvironmental Analysis. *J. Energy Resour. Technol.* **2014**, *136*, 22001. [CrossRef]
24. Hong, X.; Chen, J.; Lyu, H.; Sheng, D.; Li, W.; Li, H. Advanced exergoenvironmental evaluation for a coal-fired power plant of near-zero air pollutant emission. *Appl. Therm. Eng.* **2018**, *128*, 1139–1150. [CrossRef]
25. Morosuk, T.; Tsatsaronis, G. Advanced exergy-based methods used to understand and improve energy-conversion systems. *Energy* **2019**, *169*, 238–246. [CrossRef]

26. Boyaghchi, F.A.; Sohbatloo, A. Assessment and optimization of a novel solar driven natural gas liquefaction based on cascade ORC integrated with linear Fresnel collectors. *Energy Convers. Manag.* **2018**, *162*, 77–89. [CrossRef]
27. Ding, Y.; Liu, C.; Zhang, C.; Xu, X.; Li, Q.; Mao, L. Exergoenvironmental model of Organic Rankine Cycle system including the manufacture and leakage of working fluid. *Energy* **2018**, *145*, 52–64. [CrossRef]
28. Alibaba, M.; Pourdarbani, R.; Manesh, M.H.K.; Ochoa, G.V.; Forero, J.D. Thermodynamic, exergo-economic and exergo-environmental analysis of hybrid geothermal-solar power plant based on ORC cycle using emergy concept. *Heliyon* **2020**, *6*, e03758. [CrossRef]
29. Boyaghchi, F.A.; Chavoshi, M.; Sabeti, V. Multi-generation system incorporated with PEM electrolyzer and dual ORC based on biomass gasification waste heat recovery: Exergetic, economic and environmental impact optimizations. *Energy* **2018**, *145*, 38–51. [CrossRef]
30. Wang, W.; Wang, J.; Lu, Z.; Wang, S. Exergoeconomic and exergoenvironmental analysis of a combined heating and power system driven by geothermal source. *Energy Convers. Manag.* **2020**, *211*, 112765. [CrossRef]
31. Alibaba, M.; Pourdarbani, R.; Manesh, M.H.K.; Herrera-Miranda, I.; Gallardo-Bernal, I.; Hernández-Hernández, J.L. Conventional and advanced exergy-based analysis of hybrid geothermal-solar power plant based on ORC cycle. *Appl. Sci.* **2020**, *10*, 5206. [CrossRef]
32. Ghorbani, S.; Khoshgoftar-Manesh, M.H.; Nourpour, M.; Blanco-Marigorta, A.M. Exergoeconomic and exergoenvironmental analyses of an integrated SOFC-GT-ORC hybrid system. *Energy* **2020**, *206*, 118151. [CrossRef]
33. Ochoa, G.V.; Prada, G.; Duarte-Forero, J. Carbon footprint analysis and advanced exergo-environmental modeling of a waste heat recovery system based on a recuperative organic Rankine cycle. *J. Clean. Prod.* **2020**, *274*, 122838. [CrossRef]
34. Herrera-Orozco, I.; Valencia-Ochoa, G.; Duarte-Forero, J. Exergo-environmental assessment and multi-objective optimization of waste heat recovery systems based on Organic Rankine cycle configurations. *J. Clean. Prod.* **2021**, *288*, 125679. [CrossRef]
35. Tian, H.; Liu, P.; Shu, G. Challenges and opportunities of Rankine cycle for waste heat recovery from internal combustion engine. *Prog. Energy Combust. Sci.* **2021**, *84*, 100906. [CrossRef]
36. Shi, L.; Shu, G.; Tian, H.; Deng, S. A review of modified Organic Rankine cycles (ORCs) for internal combustion engine waste heat recovery (ICE-WHR). *Renew. Sustain. Energy Rev.* **2018**, *92*, 95–110. [CrossRef]
37. Peris, B.; Navarro-Esbrí, J.; Molés, F. Bottoming organic Rankine cycle configurations to increase Internal Combustion Engines power output from cooling water waste heat recovery. *Appl. Therm. Eng.* **2013**, *61*, 364–371. [CrossRef]
38. Hou, G.; Bi, S.; Lin, M.; Zhang, J.; Xu, J. Minimum variance control of organic Rankine cycle based waste heat recovery. *Energy Convers. Manag.* **2014**, *86*, 576–586. [CrossRef]
39. Rahbar, K.; Mahmoud, S.; Al-Dadah, R.K.; Moazami, N.; Mirhadizadeh, S.A. Review of organic Rankine cycle for small-scale applications. *Energy Convers. Manag.* **2017**, *134*, 135–155. [CrossRef]
40. Schuster, A.; Karellas, S.; Kakaras, E.; Spliethoff, H. Energetic and economic investigation of Organic Rankine Cycle applications. *Appl. Therm. Eng.* **2009**, *29*, 1809–1817. [CrossRef]
41. Invernizzi, C.; Iora, P.; Silva, P. Bottoming micro-Rankine cycles for micro-gas turbines. *Appl. Therm. Eng.* **2007**, *27*, 100–110. [CrossRef]
42. Desai, N.B.; Bandyopadhyay, S. Process integration of organic Rankine cycle. *Energy* **2009**, *34*, 1674–1686. [CrossRef]
43. Ambiente, M.D.E.; Territorial, D. Resolucion 909. 2008. Available online: https://www.minambiente.gov.co/documento-entidad/resolucion-909-del-2008/ (accessed on 1 February 2023).
44. *NFPA 704: Standard System for the Identification of the Hazards of Materials for Emergency Response, 2017 ed.*; National Fire Protection Association: Quincy, MA, USA, 2017; p. 2017.
45. Scaccabarozzi, R.; Tavano, M.; Invernizzi, C.M.; Martelli, E. Comparison of working fluids and cycle optimization for heat recovery ORCs from large internal combustion engines. *Energy* **2018**, *158*, 396–416. [CrossRef]
46. Shu, G.; Zhao, M.; Tian, H.; Huo, Y.; Zhu, W. Experimental comparison of R123 and R245fa as working fluids for waste heat recovery from heavy-duty diesel engine. *Energy* **2016**, *115*, 756–769. [CrossRef]
47. Tian, H.; Shu, G.; Wei, H.; Liang, X.; Liu, L. Fluids and parameters optimization for the organic Rankine cycles (ORCs) used in exhaust heat recovery of Internal Combustion Engine (ICE). *Energy* **2012**, *47*, 125–136. [CrossRef]
48. Lai, N.A.; Wendland, M.; Fischer, J. Working fluids for high-temperature organic Rankine cycles. *Energy* **2011**, *36*, 199–211. [CrossRef]
49. Weith, T.; Heberle, F.; Preißinger, M.; Brüggemann, D. Performance of Siloxane Mixtures in a High-Temperature Organic Rankine Cycle Considering the Heat Transfer Characteristics during Evaporation. *Energies* **2014**, *7*, 5548–5565. [CrossRef]
50. Spinelli, A.; Cammi, G.; Zocca, M.; Gallarini, S.; Cozzi, F.; Gaetani, P.; Dossena, V.; Guardone, A. Experimental observation of non-ideal expanding flows of Siloxane MDM vapor for ORC applications. *Energy Procedia* **2017**, *129*, 1125–1132. [CrossRef]
51. Invernizzi, C.M.; Iora, P.; Manzolini, G.; Lasala, S. Thermal stability of n-pentane, cyclo-pentane and toluene as working fluids in organic Rankine engines. *Appl. Therm. Eng.* **2017**, *121*, 172–179. [CrossRef]
52. Secretariat, O. United Nations Environment Programme. Synthesis of the reports of the Scientific, Environmental Effects, and Technology and Economic Assessment Panels of the Montreal Protocol—1999. 2000. Available online: https://digitallibrary.un.org/record/514339 (accessed on 1 February 2023).
53. *Kyoto Protocol to the United Nations Framework Convention On Climate Change United Nations*; UNFCC: Bonn, Germany, 1998.

54. Invernizzi, C.M.; Bonalumi, D. *Thermal Stability of Organic Fluids for Organic Rankine Cycle Systems*; Elsevier Ltd.: Amsterdam, The Netherlands, 2017. [CrossRef]
55. Lemmon, E.; Huber, M.; McLinden, M. *NIST Standard Reference Database 23: Reference Fluid Thermodynamic and Transport Properties-REFPROP, Version 8.0*; Natl. Std. Ref. Data Series (NIST NSRDS); National Institute of Standards and Technology: Gaithersburg, MD, USA, 2007.
56. Valencia, G.; Fontalvo, A.; Cárdenas, Y.; Duarte, J.; Isaza, C. Energy and exergy analysis of different exhaust waste heat recovery systems for natural gas engine based on ORC. *Energies* **2019**, *12*, 2378. [CrossRef]
57. Kelly, S. Energy Systems Improvement Based on Endogenous and Exogenous Exergy Destruction. Ph.D. Thesis, Technische Universität Berlin, Berlin, Germany, 2008. [CrossRef]
58. Tsatsaronis, G.; Park, M.H. On avoidable and unavoidable exergy destructions and investment costs in thermal systems. *Energy Convers. Manag.* **2002**, *43*, 1259–1270. [CrossRef]
59. Kelly, S.; Morozyuk, T. Endogenous and Exogenous Exergy Destruction in Thermal Systems. *ASME Int. Mech. Eng. Congr. Expos.* **2006**, *47640*, 311–317. [CrossRef]
60. International Organization for Standardization. *Environmental Management The ISO 14000 Family of International Standards ISO in Brief ISO and the Environment*; International Organization for Standardization: Geneva, Switzerland, 2009.
61. Liu, C.; He, C.; Gao, H.; Xie, H.; Li, Y.; Wu, S.; Xu, J. The environmental impact of organic Rankine cycle for waste heat recovery through life-cycle assessment. *Energy* **2013**, *56*, 144–154. [CrossRef]
62. Valencia, G.; Núñez, J.; Duarte, J. Multiobjective optimization of a plate heat exchanger in a waste heat recovery organic rankine cycle system for natural gas engines. *Entropy* **2019**, *21*, 655. [CrossRef] [PubMed]
63. Petrakopoulou, F.; Tsatsaronis, G.; Morosuk, T.; Carassai, A. Conventional and advanced exergetic analyses applied to a combined cycle power plant. *Energy* **2012**, *41*, 146–152. [CrossRef]
64. Shu, G.; Li, X.; Tian, H.; Liang, X.; Wei, H.; Wang, X. Alkanes as working fluids for high-temperature exhaust heat recovery of diesel engine using organic Rankine cycle. *Appl. Energy* **2014**, *119*, 204–217. [CrossRef]